

# Practical Hybrid Beamforming for Millimeter Wave Massive MIMO Full Duplex with Limited Dynamic Range

Chandan Kumar Sheemar, *Student Member, IEEE*, Christo Kurisummoottil Thomas, *Member, IEEE*,  
and Dirk Slock, *Fellow, IEEE*

In this paper, we present a novel hybrid beamforming (HYBF) design to maximize the weighted sum-rate (WSR) in a single-cell millimeter-wave (mmWave) massive multiple-input-multiple-output (MIMO) full duplex (FD) system. Compared to the traditional HYBF designs, we consider the joint sum-power and the practical per-antenna power constraints. The multi-antenna users and the hybrid FD base station (BS) are assumed to be suffering from the limited dynamic range (LDR) noise due to non-ideal hardware. The traditional LDR noise model is first extended to the mmWave and an impairment-aware HYBF approach is adopted. A novel interference, self-interference (SI) and LDR aware optimal power allocation scheme for the multi-antenna uplink (UL) users and the hybrid FD BS is also presented. The analog processing stage is assumed to be quantized, and both the unit-modulus and the unconstrained cases are studied. The maximum achievable gain of a multi-user mmWave FD system over a fully digital half duplex (HD) system with different levels of the LDR noise variance and different numbers of the radio-frequency (RF) chains is investigated. Simulation results show that the proposed HYBF design outperforms the fully digital HD system with only a few RF chains at any LDR noise level. The advantage of having amplitude control at the analog stage is also examined and additional gain is evident when the number of RF chains at the FD BS is small.

**Index Terms**—Millimeter wave Full Duplex, Hybrid Beamforming, Limited Dynamic Range, Minorization-Maximization

## I. INTRODUCTION

THE revolution in wireless communications has led to an exponential increase in the data rate requirements and users' number. Millimeter-wave (mmWave) frequency band 30 – 300 GHz can accommodate the ever-increasing data demands and results to be a vital resource for the future wireless communications [1]. It offers much wider bandwidths than the traditional cellular networks, and the available spectrum at such higher frequencies is 200 times greater [2]. Full duplex (FD) communication in mmWave has the potential to double the spectral efficiency compared to a half duplex (HD) system, as it enables simultaneous transmission and reception in the same frequency band. Moreover, it can be beneficial for efficient management of the available spectrum, reducing end-to-end delays/latency, solving the hidden node problem, and enabling joint communication and sensing [3]–[6].

Self-interference (SI) is a key challenge to deal with, which can be 90 – 110 dB higher than the received signal [7], [8]. Given the tremendous amount of SI, signal reception is impossible without a proper SI cancellation (SIC) scheme. Beamforming is a potential tool to jointly mitigate the SI and serve multiple users [9]–[18]. However, the achievable gain with beamforming in practical communication systems is limited by the limited dynamic range (LDR) of the radio-frequency (RF) chains. The signal suffers from LDR noise due to the distortions introduced by non-ideal power amplifiers (PAs), analog-to-digital-converters (ADCs), digital-to-analog-converters, mixers and low noise PAs. For the fully digital FD systems, LDR noise can be modelled with the well-established noise model available in [10]–[18], which enables designing impairment aware beamforming. In general, impairment aware

beamforming designs are much more robust to the distortions and can significantly outperform the naive schemes [19], [20], see, e.g., [20, Figure 2].

### A. State-of-the-art and Motivation

Traditional multiple-input-multiple-output (MIMO) FD systems, e.g., for sub-6GHz, are based on digital beamforming. In the mmWave band, the FD base stations (BSs) need to be equipped with a massive number of antennas to overcome the propagation challenges. Due to the hardware cost, they will have to rely on a hybrid architecture, consisting of only a few RF chains. Therefore, efficient hybrid beamforming (HYBF) schemes are required for such transceivers to manage interference by performing large-dimensional phasor processing in the analog domain and lower-dimensional digital processing [21]–[37].

In [22], a single stream HYBF for two bidirectional massive MIMO (mMIMO) FD nodes is studied. In [23], HYBF for a FD relay assisted mmWave macro-cell scenario is investigated. In [24], HYBF for two mmWave mMIMO bidirectional FD nodes is presented. In [38], HYBF for FD integrated access and backhaul is presented. In [25], the authors have proposed an HYBF scheme for a point-to-point FD communication. A novel HYBF design for an FD mmWave mMIMO relay is proposed in [26]. HYBF for a bidirectional point-to-point OFDM FD system is presented in [28]. In [29], the authors study a modified zero-forcing max-power design with HYBF for two mMIMO FD nodes. In [30], HYBF for a multi-cell mmWave FD with single antenna users is presented. In [31], a low-cost phasor design for HYBF in a single-cell mmWave FD system with single-antenna users is proposed. In [32], HYBF for mmWave FD with one uplink (UL) and one downlink (DL) multi-antenna HD user, only under the receive side LDR is proposed. In [33], HYBF for two mMIMO nodes to simultaneously maximize the sum spectral efficiency

Chandan Kumar Sheemar and Dirk Slock are with the communication systems department at EURECOM, Sophia Antipolis, 06410, France (emails:sheemar@eurecom.fr,slock@eurecom.fr);

Christo Kurisummoottil Thomas is with Qualcomm Finland RFFE Oy, Keilaranta 8, 02150 Espoo (e-mail: ckurisum@qti.qualcomm.com).

and cancel the SI in the analog domain by keeping the signal level at the input of the ADCs under control is proposed. In [34], HYBF for two fully connected nodes that approaches SI-free sum-spectral efficiency is proposed. In [35], HYBF for mmWave FD equipped with analog SI cancellation stage is presented. In [36], HYBF for a point-to-point mmWave FD mMIMO K-pair interference channel is presented. Frequency-selective HYBF for a wide-band mmWave FD systems is studied in [37].

The literature on the multi-antenna multi-user mmWave FD systems [32], [34], [35], [37] is limited only to the case of one UL and one DL user. In [32], the receive side LDR is also considered, which is dominated by the quantization noise of the ADCs. However, the LDR at the transmit side is ignored, which also affects the performance of FD systems [39]. The effect of cross-interference generated from the UL user towards the DL user is also not considered in [32], which can have a major impact on the achievable performance. Cross-interference generated from the neighbouring cells is well investigated in the dynamic time-division-duplexing networks [40]–[44], and it is more harmful for the multi-user FD systems as it occurs in the same cell. For example, consider the case of a small cell, in which BSs and users are expected to operate with a similar amount of transmit power [44]. Suppose that one FD BS simultaneously serves one UL and one DL user and that both the users are located close to each other and sufficiently far from the BS. In such a case, cross-interference can become as severe as the SI and can completely drown the useful signal intended for the DL user if not considered in the beamforming design. In a multi-user scenario with multiple UL users located near the DL users, each DL user suffers from cross-interference, which is summed over all the UL users' transmit power, with each UL user transmitting with a similar amount of power as the BS. In such a case, cross-interference can become even more severe than the SI if not considered in the design.

### B. Main Contributions

We present a novel HYBF design to maximize the weighted sum-rate (WSR) in a single-cell mmWave FD system with multi-antenna users. Our design relies on alternating optimization and uses the mathematical tools offered by the minorization-maximization method [45]. The multi-antenna HD users and the hybrid FD BS are assumed to be suffering from the LDR noise, which is modelled with the traditional LDR model [12] and by extending it to the case of a hybrid transceiver, respectively. Our work presents the first analysis of a mmWave FD system suffering from the LDR noise.

In contrast to the traditional HYBF designs for mmWave FD, in this work, the beamformers are designed under the joint sum-power and the practical per-antenna power constraints. The sum-power constraint at each terminal is imposed by the regulations, which limits its total transmit power. In practice, each transmit antenna is equipped with its PA<sup>1</sup> [47] and the per-antenna power constraints arise due to the power

consumption limits imposed on the physical PAs [47]–[51]. An optimal SI, interference and LDR aware power allocation scheme is also presented to satisfy the joint constraints. Compared to the digital part, designing the analog part is more challenging as it must obey the unit-modulus constraint. Recently, new transceivers have started to emerge, which with the aid of amplitude modulators (AMs), also allow amplitude control for the analog stage [32], [52], [53]. Such transceivers alleviate the unit-modulus constraint but require additional hardware. Hence, we study both the unit-modulus and the AMs cases and investigate when the amplitude control for the mmWave FD systems can be advantageous. In practice, as the analog beamformer and the analog combiner can assume only finite values, a quantization constraint is also imposed on the analog part. The WSR does not depend on the digital combiners in our problem formulation. Therefore, they are omitted in the optimization problem and must be chosen as the minimum-mean-squared-error (MMSE) combiners after the convergence of the proposed algorithm. Our HYBF design has to optimize only the digital beamformers for the UL and the DL users and the analog beamformer and combiner for the mmWave FD BS. By omitting the digital combiners, equal to the sum of the number of UL and DL users, the HYBF design simplifies and the per-iteration computational complexity reduces significantly.

Simulation results show that our design outperforms a fully digital HD system and can deal with the SI, interference and cross-interference with only a few RF chains. Results are reported with different LDR noise levels, and significant performance gain is observed at any level.

In summary, the contributions of our work are:

- Extension of the LDR noise model for a hybrid FD transceiver.
- Introduction of the WSR maximization problem formulation for HYBF in a single-cell mmWave mMIMO FD system affected by the LDR noise.
- A novel LDR and the practical per-antenna power constraints aware HYBF design.
- Investigation of the achievable WSR in a multi-user mmWave FD system as function of the LDR noise.
- Optimal interference, SI and LDR aware power allocation scheme for the hybrid FD BS and the UL users.

**Notations:** Boldface lower and upper case characters denote vectors and matrices, respectively.  $\mathbb{E}\{\cdot\}$ ,  $\text{Tr}\{\cdot\}$ ,  $(\cdot)^H$ ,  $(\cdot)^T$ ,  $\otimes$ ,  $\mathbf{I}$ ,  $\mathbf{D}_d$  and  $i$  denote expectation, trace, conjugate transpose, transpose, Kronecker product, identity matrix,  $d$  dominant vectors selection matrix and the imaginary unit, respectively.  $\text{vec}(\mathbf{X})$  stacks the columns of  $\mathbf{X}$  into a vector  $\mathbf{x}$  and  $\text{unvec}(\mathbf{x})$  reshapes  $\mathbf{x}$  into  $\mathbf{X}$ .  $\angle \mathbf{X}$  and  $\angle \mathbf{x}$  return the unit-modulus phasors of  $\mathbf{X}$  and the unit-modulus phasor of  $\mathbf{x}$ , respectively.  $\text{Cov}(\cdot)$  and  $\text{diag}(\cdot)$  denote the covariance and diagonal matrices, respectively.  $\text{SVD}(\mathbf{X})$  returns the singular value decomposition (SVD) of  $\mathbf{X}$ . Element of  $\mathbf{X}$  at the  $m$ -th row and  $n$ -th column is denoted with  $\mathbf{X}(m, n)$ . Vector of zeros of size  $M$  is denoted with  $\mathbf{0}_{M \times 1}$ . Operators  $|\mathbf{X}|$  and  $|x|$  return a matrix of moduli of  $\mathbf{X}$  and the modulus of scalar  $x$ , respectively.

<sup>1</sup>The mMIMO systems are also expected to be deployed with one PA per-antenna to enable the deployment of very low-cost PAs [46].

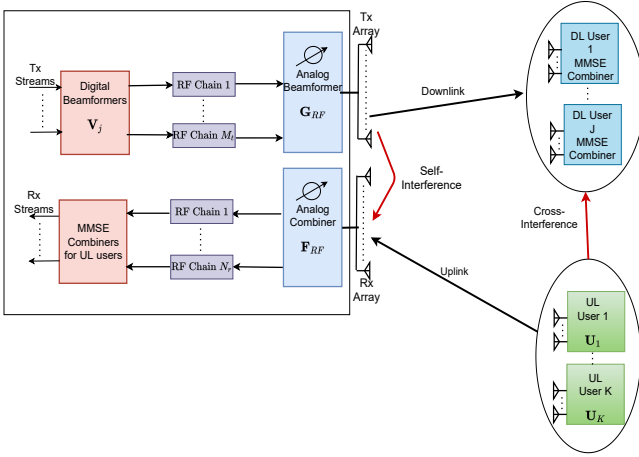


Fig. 1: Full Duplex in mmWave with hybrid beamforming and combining. Tx and Rx denote transmit and receive, respectively.

**Paper Organization:** The rest of the paper is organized as follows. Section II presents the system model, problem formulation and extends the LDR noise model. Sections III and IV present the minorization-maximization method and a novel HYBF design, respectively. Finally, Sections V and VI present the simulation results and conclusions, respectively.

## II. SYSTEM MODEL

We consider a single-cell mmWave FD system consisting of one hybrid FD BS serving  $J$  DL and  $K$  UL fully digital multi-antenna users, as shown in Fig. 1. We assume perfect channel state information (CSI)<sup>2</sup>. The FD BS is assumed to have  $M_t$  transmit and  $N_r$  receive RF chains, and  $M_0$  transmit and  $N_0$  receive antennas. Let  $\mathcal{U} = \{1, \dots, K\}$  and  $\mathcal{D} = \{1, \dots, J\}$  denote the sets containing the indices of the UL and the DL users, respectively. Let  $M_k$  and  $N_j$  denote the number of transmit and receive antennas for the  $k$ -th UL and the  $j$ -th DL user, respectively. We consider a multi-stream approach and the number of data streams transmitted from the  $k$ -th UL and to the  $j$ -th DL user are denoted as  $u_k$  and  $v_j$ , respectively. Let  $\mathbf{U}_k \in \mathbb{C}^{M_k \times u_k}$  and  $\mathbf{V}_j \in \mathbb{C}^{M_t \times v_j}$  denote the precoders for the white unitary variance data streams  $\mathbf{v}_k \in \mathbb{C}^{u_k \times 1}$  and  $\mathbf{v}_j \in \mathbb{C}^{v_j \times 1}$ , respectively. Let  $\mathbf{G}_{RF} \in \mathbb{C}^{M_0 \times M_t}$  and  $\mathbf{F}_{RF} \in \mathbb{C}^{N_0 \times N_r}$  denote the fully connected analog beamformer and combiner at the FD BS, respectively. Let  $\mathcal{P} = \{1, e^{i2\pi/n_{ps}}, \dots, e^{i2\pi(n_{ps}-1)/n_{ps}}\}$  denote the set of  $n_{ps}$  possible discrete values that the phasors at the analog stage can assume on the unit-circle. For HYBF with the unit-modulus constraint, we define the quantizer function  $\mathbb{Q}_P(\cdot)$  to quantize the unit-modulus phasors of the analog beamformer and combiner such that  $\mathbb{Q}_P(\angle \mathbf{G}_{RF}(m, n)) \in \mathcal{P}$  and  $\mathbb{Q}_P(\angle \mathbf{F}_{RF}(m, n)) \in \mathcal{P}$ ,  $\forall m, n$ . For HYBF with amplitude control, the phase part is still quantized with  $\mathbb{Q}_P(\cdot)$  and belongs to  $\mathcal{P}$ . Let  $\mathcal{A} = \{a_0, \dots, a_{A-1}\}$  denote the set of  $A$  possible values that the AMs can assume. Let  $\mathbb{Q}_A(\cdot)$  denote the quantizer function to quantize the amplitudes of  $\mathbf{G}_{RF}$  and  $\mathbf{F}_{RF}$

such that  $\mathbb{Q}_A(|\mathbf{G}_{RF}(m, n)|) \in \mathcal{A}$  and  $\mathbb{Q}_A(|\mathbf{F}_{RF}(m, n)|) \in \mathcal{A}$ ,  $\forall m, n$ . A complex number  $\mathbf{G}_{RF}(m, n)$  with amplitude in  $\mathcal{A}$  and phase part in  $\mathcal{P}$  can be written as  $\mathbf{G}_{RF}(m, n) = \mathbb{Q}_A(|\mathbf{G}_{RF}(m, n)|)\mathbb{Q}_P(\angle \mathbf{G}_{RF}(m, n))$ . The thermal noise vectors at the FD BS and at the  $j$ -th DL user are denoted with  $\mathbf{n}_0 \sim \mathcal{CN}(0, \sigma_0^2 \mathbf{I}_{N_0})$  and  $\mathbf{n}_j \sim \mathcal{CN}(0, \sigma_j^2 \mathbf{I}_{N_j})$ , respectively. Let  $\mathbf{c}_k$  and  $\mathbf{e}_j$  denote the LDR noise vector for the  $k$ -th UL and the  $j$ -th DL user, respectively, which can be modelled as [12]

$$\mathbf{c}_k \sim \mathcal{CN}(\mathbf{0}_{M_k \times 1}, k_k \text{diag}(\mathbf{U}_k \mathbf{U}_k^H)), \quad (1)$$

$$\mathbf{e}_j \sim \mathcal{CN}(\mathbf{0}_{N_j \times 1}, \beta_j \text{diag}(\mathbf{\Phi}_j)), \quad (2)$$

where  $k_k \ll 1$ ,  $\beta_j \ll 1$ ,  $\mathbf{\Phi}_j = \text{Cov}(\mathbf{r}_j)$  and  $\mathbf{r}_j$  denotes the undistorted signal received by the DL user  $j \in \mathcal{D}$ . Let  $\mathbf{c}_0$  and  $\mathbf{e}_0$  denote the LDR noise vectors in transmission and reception at the hybrid FD BS, respectively, which can be modelled as

$$\mathbf{c}_0 \sim \mathcal{CN}(\mathbf{0}_{M_0 \times 1}, k_0 \text{diag}(\sum_{n \in \mathcal{D}} \mathbf{G}_{RF} \mathbf{V}_n \mathbf{V}_n^H \mathbf{G}_{RF}^H)), \quad (3)$$

$$\mathbf{e}_0 \sim \mathcal{CN}(\mathbf{0}_{N_r \times 1}, \beta_0 \text{diag}(\mathbf{\Phi}_0)), \quad (4)$$

where  $k_0 \ll 1$ ,  $\beta_0 \ll 1$ ,  $\mathbf{\Phi}_0 = \text{Cov}(\mathbf{r}_0)$  and  $\mathbf{r}_0$  denotes the undistorted signal received by the FD BS after the analog combiner  $\mathbf{F}_{RF}$ . Note that (3) extends the transmit LDR noise model from [12] to the case of a hybrid transmitter. For the hybrid receiver at the mmWave FD BS, the ADCs, the most dominant source of the receive LDR noise, are placed after the analog combiner. Therefore,  $\mathbf{e}_0$  in (4) considers the undistorted signal received after the analog combiner. We remark that (3)-(4) is a simplified LDR noise model for a hybrid FD transceiver. There could be some correlation in practice as some circuitry is shared among multiple antennas.

The signals received at the FD BS after the analog combiner and at the  $j$ -th DL user can be written as

$$\begin{aligned} \mathbf{y} = & \mathbf{F}_{RF}^H \sum_{k \in \mathcal{U}} \mathbf{H}_k \mathbf{U}_k \mathbf{s}_k + \mathbf{F}_{RF}^H \sum_{k \in \mathcal{U}} \mathbf{H}_k \mathbf{U}_k \mathbf{c}_k + \mathbf{F}_{RF}^H \mathbf{n}_0 \\ & + \mathbf{F}_{RF}^H \mathbf{H}_0 \sum_{j \in \mathcal{D}} \mathbf{G}_{RF} \mathbf{V}_j \mathbf{s}_j + \mathbf{F}_{RF}^H \mathbf{H}_0 \mathbf{c}_0 + \mathbf{e}_0, \end{aligned} \quad (5)$$

$$\begin{aligned} \mathbf{y}_j = & \mathbf{H}_j \sum_{n \in \mathcal{D}} \mathbf{G}_{RF} \mathbf{V}_n \mathbf{s}_n + \mathbf{H}_j \sum_{n \in \mathcal{D}} \mathbf{G}_{RF} \mathbf{V}_n \mathbf{c}_0 + \mathbf{e}_j + \mathbf{n}_j \\ & + \sum_{k \in \mathcal{U}} \mathbf{H}_{j,k} \mathbf{U}_k \mathbf{s}_k + \sum_{k \in \mathcal{U}} \mathbf{H}_{j,k} \mathbf{c}_k. \end{aligned} \quad (6)$$

Matrices  $\mathbf{H}_k \in \mathbb{C}^{N_0 \times M_k}$  and  $\mathbf{H}_j \in \mathbb{C}^{N_j \times M_0}$  denote the channel response from the UL user  $k$  to the BS and from the BS to the DL user  $j$ , respectively.  $\mathbf{H}_0 \in \mathbb{C}^{N_0 \times M_0}$  and  $\mathbf{H}_{j,k} \in \mathbb{C}^{N_j \times M_k}$  denote the SI channel response for the FD BS and the cross-interference channel response from the UL  $k$  to the DL  $j$  user, respectively. At the mmWave, the channel response  $\mathbf{H}_k$  can be modelled as [25]

$$\mathbf{H}_k = \sqrt{\frac{M_k N_0}{N_c N_p}} \sum_{n_c=1}^{N_c} \sum_{n_p=1}^{N_p} \alpha_k^{(n_p, n_c)} \mathbf{a}_r(\phi_k^{(n_p, n_c)}) \mathbf{a}_t^T(\theta_k^{(n_p, n_c)}), \quad (7)$$

where  $N_c$  and  $N_p$  denote the number of clusters and the

<sup>2</sup>The CSI of the mmWave FD systems can be acquired similarly as in [54] for the mmWave HD system and it is part of the ongoing research [55].

TABLE I: Notations

$M_t$	Number of transmit RF chains for the BS
$N_r$	Number of receive RF chains for the FD BS
$M_0$	Number of transmit antennas for the BS
$N_0$	Number of receive antennas for the BS
$M_k$	Number of transmit antennas for UL user $k$
$N_j$	Number of receive antennas for DL user $j$
$\mathbf{U}_k$	Digital beamformer for UL user $k$
$\mathbf{V}_j$	Digital beamformer for DL user $j$
$\mathbf{G}_{RF}$	Analog beamformer for the FD BS
$\mathbf{F}_{RF}$	Analog combiner for the FD BS
$\mathbf{c}_k$	Transmit LDR noise from UL user $k$
$\mathbf{c}_0$	Transmit LDR noise from the FD BS
$\mathbf{e}_0$	Receive LDR noise at the FD BS
$\mathbf{e}_j$	Receive LDR noise at the DL user $j$
$\mathbf{n}_0$	Thermal noise at the FD BS
$\mathbf{n}_j$	Thermal noise at the DL user $j$
$\mathbf{H}_0$	SI channel
$\mathbf{H}_k$	Channel between the BS and UL user $k$
$\mathbf{H}_j$	Channel between the BS and DL user $j$
$\mathbf{H}_{j,k}$	Cross-interference channel between UL user $k$ and DL user $j$ .

number of rays (Figure 1 [25]), respectively, and  $\alpha_k^{(n_p, n_c)} \sim \mathcal{CN}(0, 1)$  denotes a complex Gaussian random variable whose amplitude and phase are Rayleigh and uniformly distributed, respectively. The vectors  $\mathbf{a}_r(\phi_k^{n_p, n_c})$  and  $\mathbf{a}_t^T(\theta_k^{n_p, n_c})$  denote the receive and the transmit antenna array response with the angle of arrival (AoA)  $\phi_k^{n_p, n_c}$  and the angle of departure (AoD)  $\theta_k^{n_p, n_c}$ , respectively. The channel matrices  $\mathbf{H}_j$  and  $\mathbf{H}_{j,k}$  can be modelled similarly as in (7). The SI channel can be modelled as [25]

$$\mathbf{H}_0 = \sqrt{\frac{\kappa}{\kappa+1}} \mathbf{H}_{LoS} + \sqrt{\frac{1}{\kappa+1}} \mathbf{H}_{ref}, \quad (8)$$

where  $\kappa$  denotes the Rician factor, and the matrices  $\mathbf{H}_{LoS}$  and  $\mathbf{H}_{ref}$  denote the line-of-sight (LoS) and reflected contributions for the SI channel, respectively. The channel matrix  $\mathbf{H}_{ref}$  can be modelled as (7) and the element at the  $m$ -th row and  $n$ -th columns of  $\mathbf{H}_{LoS}$  can be modelled as [25]

$$\mathbf{H}_{LoS}(m, n) = \frac{\rho}{r_{m,n}} e^{-i2\pi \frac{r_{m,n}}{\lambda}}. \quad (9)$$

where  $\rho$  denotes the power normalization constant to assure  $\mathbb{E}(\|\mathbf{H}_{LoS}(m, n)\|_F^2) = M_0 N_0$  and  $\lambda$  denotes the wavelength. The scalar  $r_{m,n}$  denotes the distance between the  $m$ -th receive and  $n$ -th transmit antenna, which depends on the transmit and receive array geometry (9) [25]. All the aforementioned notations are summarized in Table I.

Let  $\bar{k}$  and  $\bar{j}$  denote the indices in the set  $\mathcal{U}$  and  $\mathcal{D}$ , without the element  $k$  and  $j$ , respectively. The received (signal plus) interference and noise covariance matrices from the UL user  $k \in \mathcal{U}$  after the analog combiner  $\mathbf{F}_{RF}$  and at the DL user  $j \in \mathcal{D}$  are denoted as  $(\mathbf{R}_k) \mathbf{R}_{\bar{k}}$  and  $(\mathbf{R}_j) \mathbf{R}_{\bar{j}}$ , respectively. Let  $\mathbf{T}_k, \forall k \in \mathcal{U}$ , and  $\mathbf{Q}_j, \forall j \in \mathcal{D}$ , defined as

$$\mathbf{T}_k = \mathbf{U}_k \mathbf{U}_k^H, \quad (10a)$$

$$\mathbf{Q}_j = \mathbf{G}_{RF} \mathbf{V}_j \mathbf{V}_j^H \mathbf{G}_{RF}^H, \quad (10b)$$

denote the transmit covariance matrices from the UL user  $k \in \mathcal{U}$  and the DL user  $j \in \mathcal{D}$ , respectively. By considering the distortions from non-ideal hardware with the extended LDR noise model, cross-interference, interference and SI, the received covariance matrices at the BS after the analog combiner, i.e.,  $\mathbf{R}_k$  and  $\mathbf{R}_{\bar{k}}$ , and at the DL user  $j \in \mathcal{D}$ , i.e.,  $\mathbf{R}_j$  and  $\mathbf{R}_{\bar{j}}$ , can be written as (11), shown at the top of the next page. In (11),  $\mathbf{S}_k$  and  $\mathbf{S}_j$  denote the useful signal part received from UL user  $k$  and by DL user  $j$ , respectively. The undistorted received covariance matrices can be recovered from (11) as  $\Phi_0 = \mathbf{R}_k$ , with  $\beta_0 = 0$ , and  $\Phi_j = \mathbf{R}_j$ , with  $\beta_j = 0$ .

The WSR maximization problem with respect to the digital beamformers, analog beamformer and combiner with amplitudes in  $\mathcal{A}$  and phase part in  $\mathcal{P}$ , under the joint sum-power and the per-antenna power constraints, can be stated as

$$\max_{\mathbf{U}, \mathbf{V}, \mathbf{G}_{RF}, \mathbf{F}_{RF}} \sum_{k \in \mathcal{U}} w_k \ln \det(\mathbf{R}_{\bar{k}}^{-1} \mathbf{R}_k) + \sum_{j \in \mathcal{D}} w_j \ln \det(\mathbf{R}_{\bar{j}}^{-1} \mathbf{R}_j) \quad (12a)$$

$$\text{s.t. } \text{diag}(\mathbf{U}_k \mathbf{U}_k^H) \preceq \mathbf{\Lambda}_k, \quad \forall k \in \mathcal{U}, \quad (12b)$$

$$\text{diag}\left(\sum_{j \in \mathcal{D}} \mathbf{G}_{RF} \mathbf{V}_j \mathbf{V}_j^H \mathbf{G}_{RF}^H\right) \preceq \mathbf{\Lambda}_0, \quad (12c)$$

$$\text{Tr}(\mathbf{U}_k \mathbf{U}_k^H) \preceq \alpha_k, \quad \forall k \in \mathcal{U}, \quad (12d)$$

$$\text{Tr}\left(\sum_{j \in \mathcal{D}} \mathbf{G}_{RF} \mathbf{V}_j \mathbf{V}_j^H \mathbf{G}_{RF}^H\right) \preceq \alpha_0. \quad (12e)$$

$$\angle \mathbf{G}_{RF}(m, n) \in \mathcal{P}, \text{ and } |\mathbf{G}_{RF}(m, n)| \in \mathcal{A}, \quad \forall m, n, \quad (12f)$$

$$\angle \mathbf{F}_{RF}(i, j) \in \mathcal{P}, \text{ and } |\mathbf{F}_{RF}(i, j)| \in \mathcal{A}, \quad \forall i, j. \quad (12g)$$

The scalars  $w_k$  and  $w_j$  denote rate weights for the UL user  $k$  and the DL user  $j$ , respectively. The diagonal matrices  $\mathbf{\Lambda}_k$  and  $\mathbf{\Lambda}_0$  denote the per-antenna power constraints for the UL user  $k$  and the FD BS, respectively, and the scalars  $\alpha_k$  and  $\alpha_0$  denote their sum-power constraint. The collections of the digital UL and DL beamformers are denoted with  $\mathbf{U}$  and  $\mathbf{V}$ , respectively. For unit-modulus HYBF, the constraints in (12f) – (12g) on the amplitude part become unit-modulus.

*Remark 1:* Note that the rate achieved with (12) is not affected by the digital receivers if they are chosen to be the MMSE combiners, see e.g., (4) – (9) [56] for more details. For WSR maximization, only the analog combiner has to be considered in the optimization problem as it affects the size of the received covariance matrices from the UL users.

### III. MINORIZATION-MAXIMIZATION

Problem (12) is non-concave in the transmit covariance matrices  $\mathbf{T}_k$  and  $\mathbf{Q}_j$  due to the interference terms and searching its globally optimum solution is very challenging. In this section, we present the minorization-maximization method [45] for solving (12) to a local optimum.

The WSR maximization problem (12) is reformulated at each iteration with a concave reformulation with its minorizer, using the difference-of-convex (DC) programming [57] in

$$\begin{aligned}
\mathbf{R}_k &= \underbrace{\mathbf{F}_{RF}^H \mathbf{H}_k \mathbf{T}_k \mathbf{H}_k^H \mathbf{F}_{RF}}_{\triangleq \mathbf{S}_k} + \sum_{\substack{i \in \mathcal{U} \\ i \neq k}} \mathbf{F}_{RF}^H \mathbf{H}_i \mathbf{T}_i \mathbf{H}_i^H \mathbf{F}_{RF} + \sum_{i \in \mathcal{U}} k_i \mathbf{F}_{RF}^H \mathbf{H}_i \text{diag}(\mathbf{T}_i) \mathbf{H}_i^H \mathbf{F}_{RF} + \sigma_0^2 \mathbf{I}_{N_0} + \beta_0 \text{diag}(\Phi_0) \\
&\quad + \mathbf{F}_{RF}^H \mathbf{H}_0 \left( \sum_{n \in \mathcal{D}} \mathbf{Q}_n + k_0 \text{diag} \left( \sum_{n \in \mathcal{D}} \mathbf{Q}_n \right) \right) \mathbf{H}_0^H \mathbf{F}_{RF}, \quad (11a) \\
\mathbf{R}_j &= \underbrace{\mathbf{H}_j \mathbf{Q}_j \mathbf{H}_j^H}_{\triangleq \mathbf{S}_j} + \mathbf{H}_j \sum_{\substack{n \in \mathcal{D} \\ n \neq j}} \mathbf{Q}_n \mathbf{H}_j^H + k_0 \mathbf{H}_j \text{diag} \left( \sum_{n \in \mathcal{D}} \mathbf{Q}_n \right) \mathbf{H}_j^H + \sigma_j^2 \mathbf{I}_{N_j} + \sum_{i \in \mathcal{U}} \mathbf{H}_{j,i} \left( \mathbf{T}_i + k_i \text{diag}(\mathbf{T}_i) \right) \mathbf{H}_{j,i}^H + \beta_j \text{diag}(\Phi_j), \quad (11b) \\
\mathbf{R}_{\bar{k}} &= \mathbf{R}_k - \mathbf{S}_k, \quad \mathbf{R}_{\bar{j}} = \mathbf{R}_j - \mathbf{S}_j. \quad (11c)
\end{aligned}$$

terms of the variable to be updated, while the other variables are fixed. The WSR in (12) can be written with weighted-rate (WR) of user  $k \in \mathcal{U}$  ( $\text{WR}_k^{UL}$ ), user  $j \in \mathcal{D}$  ( $\text{WR}_j^{DL}$ ), WSR for  $\bar{k}$  ( $\text{WR}_{\bar{k}}^{UL}$ ) and  $\bar{j}$  ( $\text{WR}_{\bar{j}}^{DL}$ ) as

$$\text{WSR} = \underbrace{\text{WR}_k^{UL} + \text{WR}_{\bar{k}}^{UL}}_{\triangleq \text{WSR}^{UL}} + \underbrace{\text{WR}_j^{DL} + \text{WR}_{\bar{j}}^{DL}}_{\triangleq \text{WSR}^{DL}}, \quad (13)$$

where  $\text{WSR}^{UL}$  and  $\text{WSR}^{DL}$  denote the WSR in UL and DL, respectively. Considering the dependence on the transmitted covariance matrices, only  $\text{WR}_k^{UL}$  is concave in  $\mathbf{T}_k$ , meanwhile  $\text{WR}_{\bar{k}}^{UL}$  and  $\text{WR}_{\bar{j}}^{DL}$  are non-concave in  $\mathbf{T}_k$ , when  $\mathbf{T}_{\bar{k}}$  and  $\mathbf{Q}_j$ ,  $\forall j \in \mathcal{D}$ , are fixed. Similarly, only  $\text{WR}_j^{DL}$  is concave in  $\mathbf{Q}_j$  and non-concave in  $\text{WR}_{\bar{j}}^{DL}$  and  $\text{WR}_{\bar{k}}^{UL}$ , when  $\mathbf{Q}_{\bar{j}}$  and  $\mathbf{T}_k$ ,  $\forall k \in \mathcal{U}$ , are fixed. Since a linear function is simultaneously convex and concave, DC programming introduces the first order Taylor series expansion of  $\text{WR}_{\bar{k}}^{UL}$  and  $\text{WR}_{\bar{j}}^{DL}$  in  $\mathbf{T}_k$ , around  $\hat{\mathbf{T}}_k$  (i.e. around all  $\mathbf{T}_k$ ), and of  $\text{WR}_j^{DL}$  and  $\text{WR}_{\bar{j}}^{DL}$  in  $\mathbf{Q}_j$ , around  $\hat{\mathbf{Q}}_j$  (i.e. around all  $\mathbf{Q}_j$ ). Let  $\hat{\mathbf{T}}$  and  $\hat{\mathbf{Q}}$  denote the set containing all such  $\hat{\mathbf{T}}_k$  and  $\hat{\mathbf{Q}}_j$ , respectively. Let  $\hat{\mathbf{R}}_k(\hat{\mathbf{T}}, \hat{\mathbf{Q}})$ ,  $\hat{\mathbf{R}}_{\bar{k}}(\hat{\mathbf{T}}, \hat{\mathbf{Q}})$ ,  $\hat{\mathbf{R}}_j(\hat{\mathbf{T}}, \hat{\mathbf{Q}})$ , and  $\hat{\mathbf{R}}_{\bar{j}}(\hat{\mathbf{T}}, \hat{\mathbf{Q}})$  denote the covariance matrices  $\mathbf{R}_k$ ,  $\mathbf{R}_{\bar{k}}$ ,  $\mathbf{R}_j$  and  $\mathbf{R}_{\bar{j}}$  as a function of  $\hat{\mathbf{T}}$  and  $\hat{\mathbf{Q}}$ , respectively. The linearized tangent expressions for each communication link by computing the gradients

$$\hat{\mathbf{A}}_k = -\frac{\partial \text{WSR}_k^{UL}}{\partial \mathbf{T}_k} \Big|_{\hat{\mathbf{T}}, \hat{\mathbf{Q}}}, \quad \hat{\mathbf{B}}_k = -\frac{\partial \text{WSR}_{\bar{k}}^{DL}}{\partial \mathbf{T}_k} \Big|_{\hat{\mathbf{T}}, \hat{\mathbf{Q}}}, \quad (14a)$$

$$\hat{\mathbf{C}}_j = -\frac{\partial \text{WR}_j^{DL}}{\partial \mathbf{Q}_j} \Big|_{\hat{\mathbf{T}}, \hat{\mathbf{Q}}}, \quad \hat{\mathbf{D}}_j = -\frac{\partial \text{WR}_{\bar{j}}^{UL}}{\partial \mathbf{Q}_j} \Big|_{\hat{\mathbf{T}}, \hat{\mathbf{Q}}}, \quad (14b)$$

with respect to the transmit covariance matrices  $\mathbf{T}_k$  and  $\mathbf{Q}_j$  can be written as

$$\underline{\text{WSR}}_{\bar{k}}^{UL}(\mathbf{T}_k, \hat{\mathbf{T}}_k) = -\text{Tr} \left( (\mathbf{T}_k - \hat{\mathbf{T}}_k) \hat{\mathbf{A}}_k \right), \quad (15a)$$

$$\underline{\text{WR}}_{\bar{k}}^{DL}(\mathbf{T}_k, \hat{\mathbf{T}}_k) = -\text{Tr} \left( (\mathbf{T}_k - \hat{\mathbf{T}}_k) \hat{\mathbf{B}}_k \right), \quad (15b)$$

$$\underline{\text{WSR}}_j^{DL}(\mathbf{Q}_j, \hat{\mathbf{Q}}_j) = -\text{Tr} \left( (\mathbf{Q}_j - \hat{\mathbf{Q}}_j) \hat{\mathbf{C}}_j \right), \quad (15c)$$

$$\underline{\text{WSR}}_j^{UL}(\mathbf{Q}_j, \hat{\mathbf{Q}}_j) = -\text{Tr} \left( (\mathbf{Q}_j - \hat{\mathbf{Q}}_j) \hat{\mathbf{D}}_j \right). \quad (15d)$$

Note that the linearized tangent expressions  $\underline{\text{WSR}}_{\bar{k}}^{UL}$ ,  $\underline{\text{WR}}_{\bar{k}}^{DL}$ ,  $\underline{\text{WSR}}_j^{DL}$ , and  $\underline{\text{WSR}}_j^{UL}$  constitute a touching lower bound for  $\text{WSR}_{\bar{k}}^{UL}$ ,  $\text{WR}_{\bar{k}}^{DL}$ ,  $\text{WSR}_j^{DL}$  and

$\text{WSR}_j^{UL}$ , respectively. Hence, the DC programming approach is also a minorization-maximization approach, regardless of the restatement of the transmit covariance matrices  $\mathbf{T}_k$  and  $\mathbf{Q}_j$  as a function of the beamformers.

**Theorem 1.** *The gradients  $\hat{\mathbf{A}}_k$  and  $\hat{\mathbf{B}}_k$  which linearize  $\text{WSR}_{\bar{k}}^{UL}$  and  $\text{WR}_{\bar{k}}^{DL}$ , respectively, with respect to  $\mathbf{T}_k$ ,  $\forall k \in \mathcal{U}$ , and the gradients  $\hat{\mathbf{C}}_j$  and  $\hat{\mathbf{D}}_j$  which linearize  $\text{WSR}_j^{DL}$  and  $\text{WSR}_j^{UL}$ , respectively, with respect to  $\mathbf{Q}_j$ ,  $\forall j \in \mathcal{D}$ , with the first order Taylor series expansion are given in (16).*

*Proof.* Please see Appendix A.  $\square$

#### A. Concave Reformulation

In this section, we proceed by simplifying the non-concave WSR maximization problem (12), by using the result stated in Theorem 1. By using the gradients (16), (12) can be reformulated as (17), given at the top of the next page.

**Lemma 1.** *The WSR maximization problem (12) for a single-cell mmWave FD system with multi-antenna users reformulated at each iteration with its first-order Taylor series expansion as in (17) is a concave reformulation for each link.*

*Proof.* The optimization problem (12) restated as in (17) for each link is made of a concave part, i.e.,  $\log(\cdot)$ , and a linear part, i.e.,  $\text{Tr}(\cdot)$ . Each link has its own trace term with its gradients which are fixed. Since a linear function is simultaneously concave and non-concave, (17) results to be concave for each link.  $\square$

**Remark 2:** The WSR optimization (12) and its reformulated version (17) have the same Karush–Kuhn–Tucker (KKT) conditions and therefore any sub-optimal (optimal) solution of (17) is also sub-optimal (optimal) for (12).

Let  $\Psi_0 = \text{diag}([\psi_1, \dots, \psi_{M_0}])$  and  $\Psi_k = \text{diag}([\psi_{k,1}, \dots, \psi_{k,M_k}])$ , denote the diagonal matrices containing the Lagrange multipliers associated with the per-antenna power constraints for the FD BS and the UL user  $k$ , respectively. Let  $l_0$  and  $l_1, \dots, l_K$  denote the Lagrange multipliers associated with the sum-power constraint at the FD BS and at the  $K$  UL users, respectively. Let  $\Psi$  denote the collection of Lagrange multipliers associated with the per-antenna power constraints, i.e.,  $\Psi_0$  and  $\Psi_k, \forall k \in \mathcal{U}$ . Let  $\mathbf{L}$  denote the collection of the Lagrange multipliers associated with the sum-power constraints. Augmenting the linearized

$$\begin{aligned}\hat{\mathbf{A}}_k = \sum_{i \in \mathcal{U}, i \neq k} w_i & \left( \mathbf{H}_k^H \mathbf{F}_{RF} \left[ \hat{\mathbf{R}}_i^H(\hat{\mathbf{T}}, \hat{\mathbf{Q}})^{-1} - \hat{\mathbf{R}}_i(\hat{\mathbf{T}}, \hat{\mathbf{Q}})^{-1} - \beta_0 \text{diag} \left( \hat{\mathbf{R}}_i^H(\hat{\mathbf{T}}, \hat{\mathbf{Q}})^{-1} - \hat{\mathbf{R}}_i(\hat{\mathbf{T}}, \hat{\mathbf{Q}})^{-1} \right) \right] \mathbf{F}_{RF}^H \mathbf{H}_k \right. \\ & \left. - k_i \text{diag} \left( \mathbf{H}_k^H \mathbf{F}_{RF} \left( \hat{\mathbf{R}}_i^H(\hat{\mathbf{T}}, \hat{\mathbf{Q}})^{-1} - \hat{\mathbf{R}}_i(\hat{\mathbf{T}}, \hat{\mathbf{Q}})^{-1} \right) \mathbf{F}_{RF}^H \mathbf{H}_k \right) \right),\end{aligned}\quad (16a)$$

$$\begin{aligned}\hat{\mathbf{B}}_k = \sum_{l \in \mathcal{D}} w_l & \left( \mathbf{H}_{l,k}^H \left[ \hat{\mathbf{R}}_l^H(\hat{\mathbf{T}}, \hat{\mathbf{Q}})^{-1} - \hat{\mathbf{R}}_l(\hat{\mathbf{T}}, \hat{\mathbf{Q}})^{-1} - \beta_j \text{diag} \left( \hat{\mathbf{R}}_l^H(\hat{\mathbf{T}}, \hat{\mathbf{Q}})^{-1} - \hat{\mathbf{R}}_l(\hat{\mathbf{T}}, \hat{\mathbf{Q}})^{-1} \right) \right] \mathbf{H}_{l,k} \right. \\ & \left. - k_k \text{diag} \left( \mathbf{H}_{l,k}^H \left( \hat{\mathbf{R}}_l^H(\hat{\mathbf{T}}, \hat{\mathbf{Q}})^{-1} - \hat{\mathbf{R}}_l(\hat{\mathbf{T}}, \hat{\mathbf{Q}})^{-1} \right) \mathbf{H}_{l,k} \right) \right),\end{aligned}\quad (16b)$$

$$\begin{aligned}\hat{\mathbf{C}}_j = \sum_{n \in \mathcal{D}, n \neq j} w_n & \left( \mathbf{H}_n^H \left[ \hat{\mathbf{R}}_n^H(\hat{\mathbf{T}}, \hat{\mathbf{Q}})^{-1} - \hat{\mathbf{R}}_n(\hat{\mathbf{T}}, \hat{\mathbf{Q}})^{-1} - \beta_n \text{diag} \left( \hat{\mathbf{R}}_n^H(\hat{\mathbf{T}}, \hat{\mathbf{Q}})^{-1} - \hat{\mathbf{R}}_n(\hat{\mathbf{T}}, \hat{\mathbf{Q}})^{-1} \right) \right] \mathbf{H}_n \right. \\ & \left. - k_0 \text{diag} \left( \mathbf{H}_n^H \left( \hat{\mathbf{R}}_n^H(\hat{\mathbf{T}}, \hat{\mathbf{Q}})^{-1} - \hat{\mathbf{R}}_n(\hat{\mathbf{T}}, \hat{\mathbf{Q}})^{-1} \right) \mathbf{H}_n \right) \right),\end{aligned}\quad (16c)$$

$$\begin{aligned}\hat{\mathbf{D}}_j = \sum_{m \in \mathcal{U}} w_m & \left( \mathbf{H}_0^H \mathbf{F}_{RF} \left[ \hat{\mathbf{R}}_m^H(\hat{\mathbf{T}}, \hat{\mathbf{Q}})^{-1} - \hat{\mathbf{R}}_m(\hat{\mathbf{T}}, \hat{\mathbf{Q}})^{-1} - \beta_0 \text{diag} \left( \hat{\mathbf{R}}_m^H(\hat{\mathbf{T}}, \hat{\mathbf{Q}})^{-1} - \hat{\mathbf{R}}_m(\hat{\mathbf{T}}, \hat{\mathbf{Q}})^{-1} \right) \right] \mathbf{F}_{RF}^H \mathbf{H}_0 \right. \\ & \left. - k_0 \text{diag} \left( \mathbf{H}_0^H \mathbf{F}_{RF} \left( \hat{\mathbf{R}}_m^H(\hat{\mathbf{T}}, \hat{\mathbf{Q}})^{-1} - \hat{\mathbf{R}}_m(\hat{\mathbf{T}}, \hat{\mathbf{Q}})^{-1} \right) \mathbf{F}_{RF}^H \mathbf{H}_0 \right) \right),\end{aligned}\quad (16d)$$

$$\begin{aligned}\max_{\mathbf{U}, \mathbf{V}, \mathbf{G}_{RF}, \mathbf{F}_{RF}} & \sum_{k \in \mathcal{U}} w_k \ln \det \left( \mathbf{I} + \mathbf{U}_k^H \mathbf{H}_k^H \mathbf{F}_{RF} \mathbf{R}_k^{-1} \mathbf{F}_{RF}^H \mathbf{H}_k \mathbf{U}_k \right) - \text{Tr} \left( \mathbf{U}_k^H \left( \hat{\mathbf{A}}_k + \hat{\mathbf{B}}_k \right) \mathbf{U}_k \right) + \\ & \sum_{j \in \mathcal{D}} w_j \ln \det \left( \mathbf{I} + \mathbf{V}_j^H \mathbf{G}_{RF}^H \mathbf{H}_j^H \mathbf{R}_j^{-1} \mathbf{H}_j \mathbf{G}_{RF} \mathbf{V}_j \right) - \text{Tr} \left( \mathbf{V}_j^H \mathbf{G}_{RF}^H \left( \hat{\mathbf{C}}_j + \hat{\mathbf{D}}_j \right) \mathbf{G}_{RF} \mathbf{V}_j \right) \\ \text{s.t.} & \quad (12b) - (12g)\end{aligned}\quad (17)$$

$$\begin{aligned}\mathcal{L}(\mathbf{U}, \mathbf{V}, \mathbf{G}_{RF}, \mathbf{F}_{RF}, \boldsymbol{\Psi}, \mathbf{L}) &= \sum_{l=0}^K l_l \alpha_l + \text{Tr}(\boldsymbol{\Psi}_0 \boldsymbol{\Lambda}_0) + \sum_{u \in \mathcal{U}} \text{Tr}(\boldsymbol{\Psi}_u \boldsymbol{\Lambda}_u) \\ &+ \sum_{k \in \mathcal{U}} w_k \ln \det \left( \mathbf{I} + \mathbf{U}_k^H \mathbf{H}_k^H \mathbf{F}_{RF} \mathbf{R}_k^{-1} \mathbf{F}_{RF}^H \mathbf{H}_k \mathbf{U}_k \right) - \text{Tr} \left( \mathbf{U}_k^H \left( \hat{\mathbf{A}}_k + \hat{\mathbf{B}}_k + l_k \mathbf{I} + \boldsymbol{\Psi}_k \right) \mathbf{U}_k \right) \\ &+ \sum_{j \in \mathcal{D}} w_j \ln \det \left( \mathbf{I} + \mathbf{V}_j^H \mathbf{G}_{RF}^H \mathbf{H}_j^H \mathbf{R}_j^{-1} \mathbf{H}_j \mathbf{G}_{RF} \mathbf{V}_j \right) - \text{Tr} \left( \mathbf{V}_j^H \mathbf{G}_{RF}^H \left( \hat{\mathbf{C}}_j + \hat{\mathbf{D}}_j + l_0 \mathbf{I} + \boldsymbol{\Psi}_0 \right) \mathbf{G}_{RF} \mathbf{V}_j \right)\end{aligned}\quad (18)$$

WSR maximization problem (17) with the sum-power and the practical per-antenna power constraints, yields the Lagrangian (18), given at the top of this page. In (18), unconstrained analog beamformer and combiner are assumed and their constraints will be incorporated later.

#### IV. HYBRID BEAMFORMING AND COMBINING

This section presents a novel HYBF design for a multi-user mmWave FD system based on alternating optimization. In the following, for the sake of simplified explanation, the design of the digital beamformers, analog beamformer and analog combiner is presented into separate sub-sections. To update one variable, we assume the remaining variables to be fixed during the alternating optimization process. Information of the other variables is summarized in the gradients.

##### A. Digital Beamforming

To optimize the digital beamformers, we take the derivative of (18) with respect to the conjugate of  $\mathbf{U}_k$  and  $\mathbf{V}_j$ , which

leads to the following KKT conditions

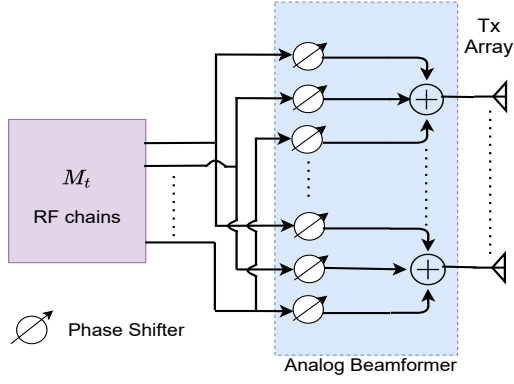
$$\begin{aligned}\mathbf{H}_k^H \mathbf{F}_{RF} \mathbf{R}_k^{-1} \mathbf{F}_{RF}^H \mathbf{H}_k \mathbf{U}_k & \left( \mathbf{I} + \mathbf{U}_k^H \mathbf{H}_k^H \mathbf{F}_{RF} \mathbf{R}_k^{-1} \mathbf{F}_{RF}^H \right. \\ & \left. \mathbf{H}_k \mathbf{U}_k \right)^{-1} - \left( \hat{\mathbf{A}}_k + \hat{\mathbf{B}}_k + \boldsymbol{\Psi}_k + l_k \mathbf{I} \right) \mathbf{U}_k = 0,\end{aligned}\quad (19a)$$

$$\begin{aligned}\mathbf{G}_{RF}^H \mathbf{H}_j^H \mathbf{R}_j^{-1} \mathbf{H}_j \mathbf{G}_{RF} \mathbf{V}_j & \left( \mathbf{I} + \mathbf{V}_j^H \mathbf{G}_{RF}^H \mathbf{H}_j^H \mathbf{R}_j^{-1} \mathbf{H}_j \mathbf{G}_{RF} \right. \\ & \left. \mathbf{V}_j \right)^{-1} - \mathbf{G}_{RF}^H \left( \hat{\mathbf{C}}_j + \hat{\mathbf{D}}_j + \boldsymbol{\Psi}_0 + l_0 \mathbf{I} \right) \mathbf{G}_{RF} \mathbf{V}_j = 0.\end{aligned}\quad (19b)$$

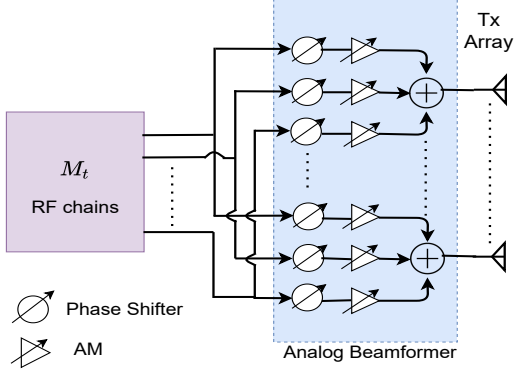
Given (19)-(19b), the digital beamformers can be optimized as stated in the following.

**Theorem 2.** *Digital beamformers  $\mathbf{U}_k$  and  $\mathbf{V}_j$ , fixed the other variables, can be optimized as the generalized dominant eigenvector solution of the pair of the following matrices*

$$\mathbf{U}_k = D_{u_k} \left( \mathbf{H}_k^H \mathbf{F}_{RF} \mathbf{R}_k^{-1} \mathbf{F}_{RF}^H \mathbf{H}_k, \hat{\mathbf{A}}_k + \hat{\mathbf{B}}_k + \boldsymbol{\Psi}_k + l_k \mathbf{I} \right) \quad (20a)$$



(a) Analog beamformer with unit-modulus phase shifters.



(b) Analog beamformer with amplitude modulators.

Fig. 2: (a) All phase shifters are unit-modulus. (b) With amplitude control.

$$\mathbf{V}_j = \mathbf{D}_{v_j} \left( \mathbf{G}_{RF}^H \mathbf{H}_j^H \mathbf{R}_j^{-1} \mathbf{H}_j \mathbf{G}_{RF}, \mathbf{G}_{RF}^H (\hat{\mathbf{C}}_j + \hat{\mathbf{D}}_j + \Psi_0 + l_0 \mathbf{I}) \mathbf{G}_{RF} \right), \quad (20b)$$

where  $\mathbf{D}_d(\mathbf{X})$  selects the  $d$  generalized dominant eigenvectors from the matrix  $\mathbf{X}$ .

*Proof.* Please see Appendix B.  $\square$

The generalized dominant eigenvector solution provides the optimized beamforming directions but not the power [57]. To include the optimal stream power allocation, we normalize the columns of the digital beamformers to unit-norm. This operation preserves the optimized beamforming directions and allows to design the optimal SI, interference and LDR aware power allocation scheme.

### B. Analog Beamforming

This section presents a novel approach to design the analog beamformer for the mmWave FD BS to maximize the WSR. The structure of the fully connected analog beamformer  $\mathbf{G}_{RF}$  is shown in Figure 2. Assuming the remaining variables to be fixed, we first consider the optimization of the unconstrained analog beamformer  $\mathbf{G}_{RF}$  as

$$\begin{aligned} \max_{\mathbf{G}_{RF}} \quad & \sum_{j \in \mathcal{D}} w_j \ln \det \left( \mathbf{I} + \mathbf{V}_j^H \mathbf{G}_{RF}^H \mathbf{H}_j^H \mathbf{R}_j^{-1} \mathbf{H}_j \mathbf{G}_{RF} \mathbf{V}_j \right) \\ & - \text{Tr} \left( \mathbf{V}_j^H \mathbf{G}_{RF}^H (\hat{\mathbf{C}}_j + \hat{\mathbf{D}}_j + l_0 \mathbf{I} + \Psi_0) \mathbf{G}_{RF} \mathbf{V}_j \right). \end{aligned} \quad (21)$$

Note that from (17) only the terms shown in (21) depend on the analog combiner  $\mathbf{G}_{RF}$  and the information about the other variables is captured in the gradients  $\hat{\mathbf{C}}_j$  and  $\hat{\mathbf{D}}_j$ . To solve (21), we take its derivative with respect to the conjugate of  $\mathbf{G}_{RF}$ , which yields the following KKT condition

$$\begin{aligned} \mathbf{H}_j^H \mathbf{R}_j^{-1} \mathbf{H}_j \mathbf{G}_{RF} \mathbf{V}_j \mathbf{V}_j^H \left( \mathbf{I} + \mathbf{V}_j \mathbf{V}_j^H \mathbf{G}_{RF}^H \mathbf{H}_j^H \mathbf{R}_j^{-1} \mathbf{H}_j \right. \\ \left. \mathbf{G}_{RF} \right)^{-1} - \left( \hat{\mathbf{C}}_j + \hat{\mathbf{D}}_j + \Psi_0 + l_0 \mathbf{I} \right) \mathbf{G}_{RF} \mathbf{V}_j \mathbf{V}_j^H = 0. \end{aligned} \quad (22)$$

Given (22), the analog beamformer  $\mathbf{G}_{RF}$  for the mmWave FD BS can be optimized as stated in the following.

**Theorem 3.** *The vectorized unconstrained analog beamformer  $\text{vec}(\mathbf{G}_{RF})$  can be optimized as one generalized dominant eigenvector solution of the pair of the following matrices*

$$\begin{aligned} \text{vec}(\mathbf{G}_{RF}) = \mathbf{D}_1 \left( \sum_{j \in \mathcal{D}} \left( \mathbf{V}_j \mathbf{V}_j^H \left( \mathbf{I} + \mathbf{V}_j \mathbf{V}_j^H \mathbf{G}_{RF}^H \mathbf{H}_j^H \mathbf{R}_j^{-1} \mathbf{H}_j \mathbf{G}_{RF} \right)^{-1} \right)^T \otimes \mathbf{H}_j^H \mathbf{R}_j^{-1} \mathbf{H}_j, \right. \\ \left. \sum_{j \in \mathcal{D}} \left( \mathbf{V}_j \mathbf{V}_j^H \right)^T \otimes \left( \hat{\mathbf{C}}_j + \hat{\mathbf{D}}_j + \Psi_0 + l_0 \mathbf{I} \right) \right), \end{aligned} \quad (23)$$

where  $\mathbf{D}_1(\mathbf{X})$  selects the first generalized dominant eigenvector from the matrix  $\mathbf{X}$ .

*Proof.* Please see Appendix B.  $\square$

Note that Theorem 3 provides the optimized vectorized unconstrained analog beamformer  $\mathbf{G}_{RF}$  and we need to reshape it with  $\text{unvec}(\text{vec}(\mathbf{G}_{RF}))$ . To satisfy the unit-modulus and the quantization constraints for  $\mathbf{G}_{RF}$ , we do  $\mathbf{G}_{RF}(m, n) = \mathbb{Q}_P(\angle \mathbf{G}_{RF}(m, n))$ ,  $\forall m, n$ . For HYBF with AMs, the columns are first scaled to be unit-norm and the quantization constraint is satisfied as  $\mathbf{G}_{RF}(m, n) = \mathbb{Q}_A(|\mathbf{G}_{RF}(m, n)|) \mathbb{Q}_P(\angle \mathbf{G}_{RF}(m, n))$ ,  $\forall m, n$ .

### C. Analog Combiner

This section presents a novel approach to design the analog combiner  $\mathbf{F}_{RF}$  for the mmWave FD BS. Its design is more straightforward than the analog beamformer. Note that the trace terms appearing in (17) have the objective to make the beamformers' update aware of the interference generated towards the other links. However,  $\mathbf{F}_{RF}$  being a combiner, does not generate any interference and therefore does not appear in the trace terms of (17). Consequently, to optimize  $\mathbf{F}_{RF}$ , we can solve the optimization problem (12) instead of using its minorized version (17). By considering the unconstrained analog combiner  $\mathbf{F}_{RF}$ , from (12) we have

$$\max_{\mathbf{F}_{RF}} \sum_{k \in \mathcal{U}} w_k \ln \det \left( \mathbf{R}_k^{-1} \mathbf{R}_k \right). \quad (24)$$

To solve (24),  $\mathbf{F}_{RF}$  has to combine the signal received at the antenna level of the mmWave FD BS but  $\mathbf{R}_k$  and  $\mathbf{R}_k^-$  represent the received covariance matrices after the analog combiner. Let  $(\mathbf{R}_k^{ant})$   $\mathbf{R}_k^{ant}$  denote the (signal-plus) interference and noise covariance matrix received at the antennas of the FD BS, which can be obtained from  $(\mathbf{R}_k)$   $\mathbf{R}_k^-$  given in (11) by omitting  $\mathbf{F}_{RF}$ . After the analog combining, we can recover  $\mathbf{R}_k$



and  $\mathbf{R}_k^-$  as  $\mathbf{R}_k = \mathbf{F}_{RF}^H \mathbf{R}_k^{ant} \mathbf{F}_{RF}$  and  $\mathbf{R}_k^- = \mathbf{F}_{RF}^H \mathbf{R}_k^{ant} \mathbf{F}_{RF}$ , respectively,  $\forall k \in \mathcal{U}$ . Problem (24) can be restated as a function of  $\mathbf{R}_k^{ant}$  and  $\mathbf{R}_k^-$  as

$$\max_{\mathbf{F}_{RF}} \sum_{k \in \mathcal{U}} \left[ w_k \ln \det \left( \mathbf{F}_{RF}^H \mathbf{R}_k^{ant} \mathbf{F}_{RF} \right) - w_k \ln \det \left( \mathbf{F}_{RF}^H \mathbf{R}_k^- \mathbf{F}_{RF} \right) \right]. \quad (25)$$

In (17), the trace term was only linear, which made the restated optimization problem concave for each link. In (25), all the terms are fully concave. To optimize  $\mathbf{F}_{RF}$ , we take the derivative with respect to the conjugate of  $\mathbf{F}_{RF}$ , which yields the following KKT condition

$$\sum_{k \in \mathcal{U}} w_k \mathbf{R}_k^{ant} \mathbf{F}_{RF} \left( \mathbf{F}_{RF}^H \mathbf{R}_k^{ant} \mathbf{F}_{RF} \right)^{-1} - \sum_{k \in \mathcal{U}} w_k \mathbf{R}_k^- \mathbf{F}_{RF} \left( \mathbf{F}_{RF}^H \mathbf{R}_k^- \mathbf{F}_{RF} \right)^{-1} = 0. \quad (26)$$

It is immediate to see from (26) that the unconstrained analog combiner can be optimized as the dominant generalized eigenvector solution of the sum of the pair of the received covariance matrices at the antenna level, i.e.,

$$\mathbf{F}_{RF} \rightarrow \mathbf{D}_{NT} \left( \sum_{k \in \mathcal{U}} w_k \mathbf{R}_k^{ant}, \sum_{k \in \mathcal{U}} w_k \mathbf{R}_k^- \right). \quad (27)$$

To satisfy the unit-modulus and the quantization constraints for  $\mathbf{F}_{RF}$ , we do  $\mathbf{F}_{RF}(m, n) = \mathbb{Q}_P(\angle \mathbf{F}_{RF}(m, n)) \in \mathcal{P}$ ,  $\forall m, n$ . If AMs are available, the columns are scaled to be unit-norm and the quantization constraint for  $\mathbf{F}_{RF}$  is satisfied as  $\mathbf{F}_{RF}(m, n) = \mathbb{Q}_A(|\mathbf{F}_{RF}(m, n)|) \mathbb{Q}_P(\angle \mathbf{F}_{RF}(m, n))$ ,  $\forall m, n$ .

#### D. Optimal Power Allocation

Given the normalized digital beamformers and the analog beamformer, the optimal power allocation can be included while searching for the Lagrange multipliers satisfying the joint sum-power and the practical per-antenna power constraints.

Let  $\Sigma_k^{(1)}$  and  $\Sigma_k^{(2)}$ ,  $\forall k \in \mathcal{U}$  and  $\Sigma_j^{(1)}$  and  $\Sigma_j^{(2)}$ ,  $\forall j \in \mathcal{D}$ , be defined as

$$\mathbf{U}_k^H \mathbf{H}_k^H \mathbf{F}_{RF} \mathbf{R}_k^{-1} \mathbf{F}_{RF}^H \mathbf{H}_k \mathbf{U}_k = \Sigma_k^{(1)}, \quad (28a)$$

$$\mathbf{U}_k^H \left( \hat{\mathbf{A}}_k + \hat{\mathbf{B}}_k + \Psi_k + l_k \mathbf{I} \right) \mathbf{U}_k = \Sigma_k^{(2)}, \quad (28b)$$

$$\mathbf{V}_j^H \mathbf{G}_{RF}^H \mathbf{H}_j^H \mathbf{R}_j^{-1} \mathbf{H}_j \mathbf{G}_{RF} \mathbf{V}_j = \Sigma_j^{(1)}, \quad (28c)$$

$$\mathbf{V}_j^H \mathbf{G}_{RF}^H \left( \hat{\mathbf{C}}_j + \hat{\mathbf{D}}_j + \Psi_0 + l_0 \mathbf{I} \right) \mathbf{G}_{RF} \mathbf{V}_j = \Sigma_j^{(2)}. \quad (28d)$$

Given (28), the optimal stream power allocation can be included based on the result stated in the following.

**Lemma 2.** *Optimal power allocation for the hybrid FD BS and the multi-antenna UL users can be obtained by multiplying  $\Sigma_j^{(1)}$  and  $\Sigma_j^{(2)}$  with the diagonal power matrix  $\mathbf{P}_j$ ,  $\forall j \in \mathcal{D}$  and  $\Sigma_k^{(1)}$  and  $\Sigma_k^{(2)}$  with the diagonal power matrix  $\mathbf{P}_k$ ,  $\forall k \in \mathcal{U}$ , respectively.*

*Proof.* The beamformers  $\mathbf{U}_k$ ,  $\mathbf{V}_k$ , are computed as the generalized dominant eigenvectors, thus making the matrices

$\Sigma_k^{(1)}$ ,  $\Sigma_k^{(2)}$ ,  $\forall k$  and  $\Sigma_j^{(1)}$ ,  $\Sigma_j^{(2)}$ ,  $\forall j$  diagonal at each iteration. Multiplying any generalized dominant eigenvector solution matrix with a diagonal matrix still yields a generalized dominant eigenvector solution. Therefore, multiplying  $\Sigma_k^{(1)}$ ,  $\Sigma_k^{(2)}$  with  $\mathbf{P}_k$ ,  $\forall k \in \mathcal{U}$  and  $\Sigma_j^{(1)}$ ,  $\Sigma_j^{(2)}$  with  $\mathbf{P}_j$ ,  $\forall j \in \mathcal{D}$  still preserves the validity of the optimized beamforming directions.  $\square$

Given the optimized beamformers and fixed the Lagrange multipliers, by using the result stated in Lemma 2 the stream power allocation optimization problems for the UL and the DL users can be formally stated as

$$\max_{\mathbf{P}_k} w_k \ln \det \left( \mathbf{I} + \Sigma_k^{(1)} \mathbf{P}_k \right) - \text{Tr} \left( \Sigma_k^{(2)} \mathbf{P}_k \right), \quad \forall k \in \mathcal{U}, \quad (29a)$$

$$\max_{\mathbf{P}_j} w_j \ln \det \left( \mathbf{I} + \Sigma_j^{(1)} \mathbf{P}_j \right) - \text{Tr} \left( \Sigma_j^{(2)} \mathbf{P}_j \right), \quad \forall j \in \mathcal{D}. \quad (29b)$$

Solving (29) leads to the following optimal power allocation scheme

$$\mathbf{P}_k = \left( w_k \left( \mathbf{U}_k^H \left( \hat{\mathbf{A}}_k + \hat{\mathbf{B}}_k + \Psi_k + l_k \mathbf{I} \right) \mathbf{U}_k \right)^{-1} - \left( \mathbf{U}_k^H \mathbf{H}_k^H \mathbf{F}_{RF} \mathbf{R}_k^{-1} \mathbf{F}_{RF}^H \mathbf{H}_k \mathbf{U}_k \right)^{-1} \right)^+, \quad (30a)$$

$$\mathbf{P}_j = \left( w_j \left( \mathbf{V}_j^H \mathbf{G}_{RF}^H \left( \hat{\mathbf{C}}_j + \hat{\mathbf{D}}_j + \Psi_0 + l_0 \mathbf{I} \right) \mathbf{G}_{RF} \mathbf{V}_j \right)^{-1} - \left( \mathbf{V}_j^H \mathbf{G}_{RF}^H \mathbf{H}_j^H \mathbf{R}_j^{-1} \mathbf{H}_j \mathbf{G}_{RF} \mathbf{V}_j \right)^{-1} \right)^+, \quad (30b)$$

where  $(\mathbf{X})^+ = \max\{\mathbf{0}, \mathbf{X}\}$ . We remark that the proposed power allocation scheme is interference, SI, cross-interference and impairments/LDR aware as it takes into account their effect in the gradients, which are updated at each iteration. Fixed the beamformers, we can search for the multipliers satisfying the joint constraints while doing water-filling for the powers. To do so, consider the dependence of the Lagrangian (18) on the multipliers and powers as

$$\begin{aligned} \mathcal{L}(\Psi, \mathbf{L}, \mathbf{P}) &= \sum_{l=0}^K l_l p_l + \text{Tr}(\Psi_0 \Lambda_0) + \sum_{u \in \mathcal{U}} \text{Tr}(\Psi_u \Lambda_u) \\ &+ \sum_{k \in \mathcal{U}} w_k \ln \det \left( \mathbf{I} + \Sigma_k^{(1)} \mathbf{P}_k \right) - \text{Tr} \left( \Sigma_k^{(2)} \mathbf{P}_k \right) \\ &+ \sum_{j \in \mathcal{D}} w_j \ln \det \left( \mathbf{I} + \Sigma_j^{(1)} \mathbf{P}_j \right) - \text{Tr} \left( \Sigma_j^{(2)} \mathbf{P}_j \right), \end{aligned} \quad (31)$$

where  $\mathbf{P}$  is the set of stream powers in UL and DL. The multipliers in  $\Psi$  and  $\mathbf{L}$  should be such that the Lagrange dual function (31) is finite and the values of the multipliers should be strictly positive. Formally, the multipliers' search problem can be stated as

$$\begin{aligned} \min_{\Psi, \mathbf{L}} \max_{\mathbf{P}} \quad & \mathcal{L}(\Psi, \mathbf{L}, \mathbf{P}), \\ \text{s.t.} \quad & \Psi, \mathbf{L} \succeq \mathbf{0}. \end{aligned} \quad (32)$$

The dual function  $\max_{\mathbf{P}} \mathcal{L}(\Psi, \mathbf{L}, \mathbf{P})$  is the pointwise supremum of a family of functions of  $\Psi, \mathbf{L}$ , it is convex [58] and the globally optimal values for  $\Psi$  and  $\mathbf{L}$  can be obtained by using any of the numerous convex optimization



techniques. In this work, we adopt the Bisection algorithm to search the multipliers. Let  $\mathcal{M}_0 = \{\lambda_0, \psi_1, \dots, \psi_{M_0}\}$  and  $\mathcal{M}_k = \{\lambda_k, \psi_{k,1}, \dots, \psi_{k,M_k}\}$  denote the sets containing the Lagrange multipliers associated with the sum-power and the practical per-antenna power constraints for the BS and the UL user  $k \in \mathcal{U}$ , respectively. Let  $\underline{\mu}_i$  and  $\overline{\mu}_i$  denote the lower and the upper bound for the search range of multiplier  $\mu_i$ , where  $\mu_i \in \mathcal{M}_0$  or  $\mu_i \in \mathcal{M}_k$ . While searching multipliers and performing water-filling for the stream powers, the UL and the DL power matrices become non-diagonal. Therefore, we consider the SVD of the power matrices to shape them as diagonal. Namely, let  $\mathbf{P}_i$  denote the power matrix for user  $i$ , where  $i \in \mathcal{U}$  or  $i \in \mathcal{D}$ . When the power matrix  $\mathbf{P}_i$  becomes non-diagonal, consider its SVD as

$$[\mathbf{U}_{P_i}, \mathbf{D}_{P_i}, \mathbf{V}_{P_i}] = \text{SVD}(\mathbf{P}_i). \quad (33)$$

where  $\mathbf{U}_{P_i}$ ,  $\mathbf{D}_{P_i}$  and  $\mathbf{V}_{P_i}$  are the left unitary, diagonal and right unitary matrices obtained with the SVD decomposition, and set  $\mathbf{P}_i = \mathbf{D}_{P_i}$  to obtain a diagonal power matrix.

For unit-modulus HYBF, the complete alternating optimization based procedure to maximize the WSR based on the minorization-maximization method is formally stated in Algorithm 1. For HYBF with AMs, the steps  $\angle \mathbf{G}_{RF}$  and  $\angle \mathbf{F}_{RF}$  must be omitted and the amplitudes of the analog beamformer and combiner must be quantized with  $\mathbb{Q}_A(\cdot)$ . Once the proposed algorithm converges, all the combiners can be chosen as the MMSE combiners which will not affect the WSR achieved with Algorithm 1 (4) – (9) [56].

### E. Convergence

In our context, the ingredients required to prove the convergence are the minorization [45], alternating or cyclic optimization [45], Lagrange dual function [58], saddle-point interpretation [58] and KKT conditions [58]. For the WSR cost function (12), we construct its minorizer as in (15a), (15b), (15c), (15d), which restates the WSR maximization as a concave problem (17) for each link. The minorizer is a touching lower bound for the original WSR problem (12), so we can write

$$\text{WSR} \geq \underline{\text{WSR}} = \underline{\text{WSR}}_k^{UL} + \underline{\text{WSR}}_k^{UL} + \underline{\text{WSR}}_j^{DL} + \underline{\text{WSR}}_j^{DL}. \quad (34)$$

The minorizer, which is concave in  $\mathbf{T}_k$  and  $\mathbf{Q}_j$ , still has the same gradient of the original WSR and hence the KKT conditions are not affected. Reparameterizing  $\mathbf{T}_k$  or  $\mathbf{Q}_j$  in terms of  $\mathbf{U}_k, \forall k \in \mathcal{U}$  and  $\mathbf{G}_{RF}$  or  $\mathbf{V}_j, \forall j \in \mathcal{D}$ , respectively, as in (10) with the optimal power matrices and adding the power constraints to the minorizer, we get the Lagrangian (18). Every alternating update of  $\mathcal{L}$  for  $\mathbf{V}_j$ ,  $\mathbf{G}_{RF}$ ,  $\mathbf{U}_k, \forall j \in \mathcal{D}, \forall k \in \mathcal{U}$  or for  $\mathbf{P}, \mathbf{\Lambda}, \mathbf{\Psi}$  leads to an increase of the WSR, ensuring convergence. For the KKT conditions, at the convergence point, the gradients of  $\mathcal{L}$  for  $\mathbf{V}_j, \mathbf{G}_{RF}, \mathbf{U}_j$  or  $\mathbf{P}$  correspond to the gradients of the Lagrangian of the original WSR (12). For fixed analog and the digital beamformers,  $\mathcal{L}$  is concave in  $\mathbf{P}$ , hence we have strong duality for the saddle point, i.e.

$$\max_{\mathbf{P}} \min_{\mathbf{L}, \mathbf{\Psi}} \mathcal{L}(\mathbf{L}, \mathbf{\Psi}, \mathbf{P}). \quad (35)$$

---

### Algorithm 1 Practical Hybrid Beamforming Design

---

**Given:** The CSI and rate weights.

**Initialize:**  $\mathbf{G}_{RF}, \mathbf{V}_j, \forall j \in \mathcal{D}$  and  $\mathbf{U}_k, \forall k \in \mathcal{U}$ .

**Set:**  $\underline{\mu}_i = 0$  and  $\overline{\mu}_i = \mu_{i_{max}} \forall i \in \mathcal{M}_0$  or  $\forall i \in \mathcal{M}_k, \forall k \in \mathcal{U}$

**Repeat until convergence**

    Compute  $\mathbf{G}_{RF}$  (23),  $\text{unvec}(\mathbf{G}_{RF})$  and  $\mathbf{G}_{RF} = \angle \mathbf{G}_{RF}$ .

    Compute  $\mathbf{F}_{RF}$  with (27), and do  $\mathbf{F}_{RF} = \angle \mathbf{F}_{RF}$ .

**for:**  $j = 1 : J$

        Compute  $\hat{\mathbf{C}}_j, \hat{\mathbf{D}}_j$  with (16)

        Compute  $\mathbf{V}_j$  with (20b) and normalize it

**end**

**Set:**  $\underline{\mu}_0 = 0$  and  $\overline{\mu}_0 = \mu_{i_{max}} \forall i \in \mathcal{M}_0$

**for:**  $\forall \mu_0 \in \mathcal{M}_0$

**Repeat until convergence**

            set  $\mu_0 = (\underline{\mu}_0 + \overline{\mu}_0)/2$

            Compute  $\hat{\mathbf{P}}_j$  with (30b)  $\forall j$

**if** constraint for  $\mu_0$  is violated

                set  $\underline{\mu}_0 = \mu_0$ ,

**else**  $\overline{\mu}_0 = \mu_0$

$[\mathbf{U}_{P_j}, \mathbf{D}_{P_j}, \mathbf{V}_{P_j}] = \text{SVD}(\hat{\mathbf{P}}_j), \forall j$

            Set  $\mathbf{P}_j = \mathbf{D}_{P_j}$  and  $\mathbf{Q}_j = \mathbf{G}_{RF} \mathbf{V}_j \mathbf{P}_j \mathbf{V}_j^H \mathbf{G}_{RF}^H, \forall j$

**for:**  $k = 1 : K$

        Compute  $\hat{\mathbf{A}}_k, \hat{\mathbf{B}}_k$  with (16)

        Compute  $\mathbf{U}_k$  with (20a) and normalize it

**Set:**  $\underline{\mu}_k = 0$  and  $\overline{\mu}_k = \mu_{i_{max}}$

**for:**  $\forall \mu_k \in \mathcal{M}_k$

**Repeat until convergence**

            set  $\mu_k = (\underline{\mu}_k + \overline{\mu}_k)/2$

            Compute  $\hat{\mathbf{P}}_k$  with (30a).

**if** constraint for  $\mu_k$  is violated

                set  $\underline{\mu}_k = \mu_k$

**else**  $\overline{\mu}_k = \mu_k$

$[\mathbf{U}_{P_k}, \mathbf{D}_{P_k}, \mathbf{V}_{P_k}] = \text{SVD}(\hat{\mathbf{P}}_k)$

            Set  $\mathbf{P}_k = \mathbf{D}_{P_k}$  and  $\mathbf{T}_k = \mathbf{U}_k \mathbf{P}_k \mathbf{U}_k^H$

    Repeat

    Quantize  $\angle \mathbf{G}_{RF}$  and  $\angle \mathbf{F}_{RF}$  ( $|\mathbf{G}_{RF}|$  and  $|\mathbf{F}_{RF}|$  with AMs)

---

Let  $\mathbf{X}^*$  and  $x^*$  denote the optimal solution for matrix  $\mathbf{X}$  or scalar  $x$  at the convergence, respectively. At the convergence point, the solution of the optimization problem

$$\min_{\mathbf{\Lambda}, \mathbf{\Psi}} \mathcal{L}(\mathbf{V}^*, \mathbf{G}^*, \mathbf{U}^*, \mathbf{P}^*, \mathbf{L}, \mathbf{\Psi}) \quad (36)$$

satisfies the KKT conditions for the powers in  $\mathbf{P}$  and the complementary slackness conditions

$$l_0^* \left( \alpha_0 - \sum_{j \in \mathcal{D}} \text{Tr}(\mathbf{G}_{RF}^* \mathbf{V}_j^* \mathbf{P}_j^* \mathbf{V}_j^{*H} \mathbf{G}_{RF}^{*H}) \right) = 0, \quad (37a)$$

$$\text{Tr}(\mathbf{\Psi}_0^* (\mathbf{P}_0 - \sum_{j \in \mathcal{D}} \text{Tr}(\mathbf{G}_{RF}^* \mathbf{V}_j^* \mathbf{P}_j^* \mathbf{V}_j^{*H} \mathbf{G}_{RF}^{*H}))) = 0, \quad (37b)$$

$$l_k^* \left( \alpha_k - \text{Tr}(\mathbf{U}_k^* \mathbf{P}_k^* \mathbf{U}_k^{*H}) \right) = 0, \quad (37c)$$

$$\text{Tr}(\mathbf{\Psi}_k^* (\mathbf{P}_k - \text{Tr}(\mathbf{U}_k^* \mathbf{P}_k^* \mathbf{U}_k^{*H}))) = 0, \quad (37d)$$

where all the individual factors in the products are non-negative and for the per-antenna power constraints  $\mathbf{\Psi}_0^*$  and

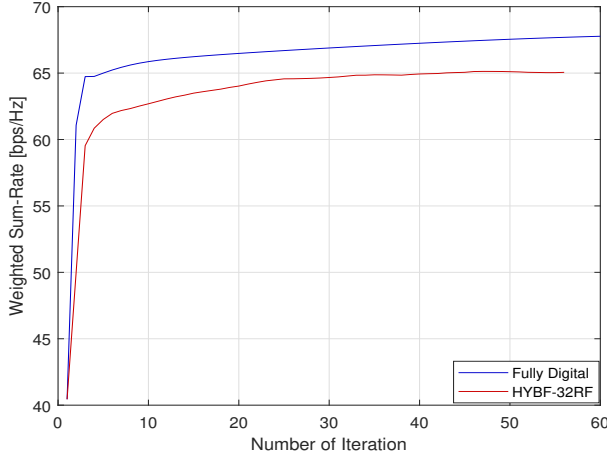


Fig. 3: Typical convergence behaviour of the proposed HYBF for the mmWave FD system.

$\Psi_k^*$ , the sum of non-negative terms being zero implies all the terms result to be zero.

*Remark 3:* The unit-modulus HYBF scheme converges to a local optimum where  $\angle \mathbf{G}_{RF}(m, n), \angle \mathbf{F}_{RF}(m, n) \in \mathcal{P}$  with  $|\mathbf{G}_{RF}(m, n)|, |\mathbf{F}_{RF}(m, n)| = 1, \forall m, n$ . Unconstrained HYBF with AMs converges to a different local optimum, where  $\angle \mathbf{G}_{RF}(m, n), \angle \mathbf{F}_{RF}(m, n) \in \mathcal{P}$  and  $|\mathbf{G}_{RF}(m, n)|, |\mathbf{F}_{RF}(m, n)| \in \mathcal{A}, \forall m, n$ . Due to quantization,  $\mathbf{G}_{RF}$  and  $\mathbf{F}_{RF}$  obtained with Algorithm 1 tend to lose their optimality and consequently achieve less WSR compared to their infinite resolution case. For unit-modulus HYBF, the loss in WSR depends only on the resolution of the phases. For HYBF with AMs, the loss in WSR depends on the resolution of both amplitudes and phases.

#### F. Complexity Analysis

In this section, we analyze the per-iteration computational complexity of the proposed HYBF design, assuming that the dimensions of the antennas get large. One iteration of Algorithm 1 updates  $K$  digital beamformers for the UL users,  $J$  digital beamformers for the DL user, one analog beamformer and one analog combiner. One dominant generalized eigenvector computation to update the analog beamformer from a matrix of size  $M_t M_0 \times M_t M_0$  in (23), is  $\mathcal{O}(M_0^2 M_t^2)$ . To update the gradients  $\hat{\mathbf{A}}_k$  and  $\hat{\mathbf{B}}_k$  for one UL user, the complexity is given by  $\mathcal{O}((K-1)N_r^3)$  and  $\mathcal{O}(JN_j^3)$ , respectively. For the gradient  $\hat{\mathbf{C}}_j$  and  $\hat{\mathbf{D}}_j$ , required to update the beamformer of the DL user  $j$ , computational complexity is  $\mathcal{O}((J-1)N_j^3)$  and  $\mathcal{O}(KN_r^3)$ , respectively. Updating the beamformer for the UL user  $k$  and the DL user  $j$  as the generalized dominant eigenvectors adds additional complexity of  $\mathcal{O}(u_k M_k^2)$  and  $\mathcal{O}(v_j N_j^2)$ , respectively. The Lagrange multipliers' update associated with the per-antenna power constraints at the FD BS or the UL users is linear in the number of antennas  $M_0$  or  $M_k$ , respectively. However, as we jointly perform the multipliers' search and the power allocation, it adds the complexity of  $\mathcal{O}(v_i^3)$ , where  $i \in \mathcal{D}$  or  $i \in \mathcal{U}$ , which can be ignored. Updating the analog combiner  $\mathbf{F}_{RF}$  for the FD BS is  $\mathcal{O}(N_r N_0^2)$ . Under the assumption that the dimensions

of the antennas are large, the per-iteration complexity is  $\approx \mathcal{O}(K^2 N_r^3 + K J N_j^3 + J^2 N_j^3 + J K N_r^3 + M_0^2 M_t^2 + N_r N_0^2)$  which depends on the number of UL and DL users served by the mmWave FD BS.

#### V. SIMULATION RESULTS

This section presents simulation results to evaluate the performance of the proposed HYBF scheme. For comparison, we define the following benchmark schemes:

a) A *Fully digital HD* scheme with LDR noise, serving the UL and the DL users by separating the resources in time. Being HD, it is neither affected by SI nor by the cross-interference.

b) A *Fully digital FD* scheme with LDR noise. This scheme sets an upper bound for the maximum achievable performance for a FD system in mmWave.

Hereafter, HYBF with the unit-modulus constraint or HYBF with AMs are denoted as HYBF-UM and HYBF-AMs, respectively. We define the signal-to-noise-ratio (SNR) for the mmWave FD system as

$$\text{SNR} = \alpha_0 / \sigma_0^2, \quad (38)$$

where the scalars  $\alpha_0$  and  $\sigma_0^2$  denote the total transmit power and the thermal noise variance at the FD BS, respectively. We set the thermal noise level for the DL users to be  $\sigma_0^2 = \sigma_j^2, \forall j$ , and the transmit power for the UL users as  $\alpha_0 = \alpha_k, \forall k$ . We consider the total transmit power normalized to 1 and choose the noise variance based on the desired SNR. To compare the gain of a FD system over a HD system, we define the additional gain in percentage as

$$\text{Gain} = \frac{WSR_{FD} - WSR_{HD}}{WSR_{HD}} \times 100 [\%], \quad (39)$$

where  $WSR_{FD}$  and  $WSR_{HD}$  denote the WSR of a FD and a HD system, respectively. To evaluate the performance, we set the per-antenna power constraints for the FD BS and the UL users as the total transmit power divided by the total number of antennas, i.e.  $\alpha_0 / M_0 \mathbf{I}$  and  $\alpha_k / M_k \mathbf{I}, \forall k$ . The BS and the multi-antenna users are assumed to be equipped with a uniform linear array (ULA) with antennas separated by half-wavelength. The transmit and the receive antenna array at the BS are assumed to be placed  $D = 20$  cm apart, with the relative angle  $\Theta = 90^\circ$ , and  $r_{m,n}$  is modelled as (9) [25]. The Rician factor  $\kappa$  for the SI channel is set to be 1. We assume that the FD BS has  $M_0 = 100$  transmit and  $N_0 = 50$  receive antennas. It serves two UL and two DL users with  $M_k = N_j = 5$  antennas and with 2 data streams for each user. The phases for both designs are quantized in the interval  $[0, 2\pi]$  with an 8-bit uniform quantizer  $\mathbb{Q}_P(\cdot)$ . For HYBF with AMs, the amplitudes are uniformly quantized with a 3-bit uniform quantizer  $\mathbb{Q}_A(\cdot)$  in the interval  $[0, a_{max}]$ , where  $a_{max} = \max\{|\max\{\mathbf{G}_{RF}\}|, \max\{|\mathbf{F}_{RF}|\}|\}$  is the maximum of the maximum modulus of  $\mathbf{G}_{RF}$  or  $\mathbf{F}_{RF}$ . We assume the same LDR noise level for all the users and the BS, i.e.  $k_0 = \beta_0 = \kappa_k = \beta_j$ . The rate-weights for all the users are set

TABLE II: Simulation parameters to simulate the multi-user mmWave FD system.

Simulation Parameters		
UL and DL users	$K, J$	2
Data streams	$v_j, u_k$	2
Antennas for the BS	$M_0, N_0$	100, 50
Clusters and Paths	$N_c, N_p$	3, 3
RF chains (BS)	$M_t = N_r$	8, 10, 16 or 32
User antennas	$M_k = N_j$	5
Rician Factor	$\kappa$	1
Tx and Rx array response	$\mathbf{a}_r, \mathbf{a}_t$	ULA, ULA
Angles	$\phi_k, \phi_j, \theta_k, \theta_j$	$\mathcal{U} \sim [-30^\circ, 30^\circ]$
Rate weights	$w_k, w_j$	1
Uniform Quantizer	$\mathcal{Q}_P(\cdot), \mathcal{Q}_A(\cdot)$	8, 3 bits
Angle between Tx and Rx array (BS)	$\Theta$	$90^\circ$
Antenna array separation (BS)	$D$	20 cm
Per-antenna power constraint	$\Lambda_k, \Lambda_0$	$\alpha_k/M_k \mathbf{I}, \alpha_0/M_0 \mathbf{I}$

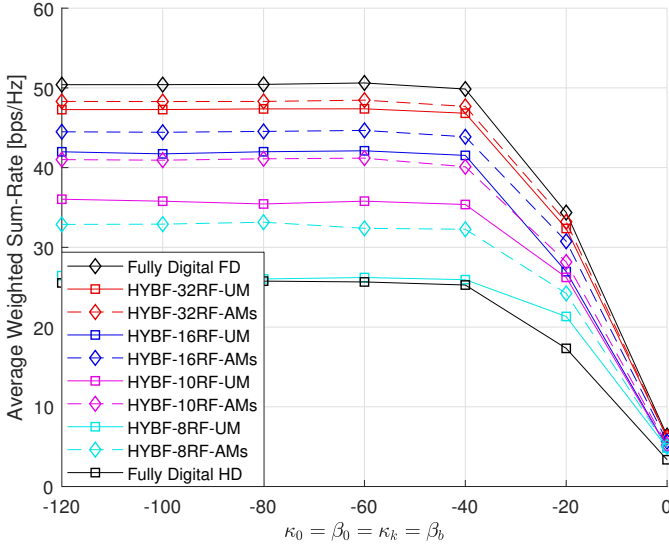


Fig. 4: Average WSR as a function of the LDR noise with SNR = 0 dB.

to be 1. All the simulation parameters are summarized in Table II. The digital beamformers are initialized as the dominant eigenvectors of the channel covariance matrices of the intended users. Analog beamformer and combiner are initialized as the dominant eigenvectors of the sum of channel covariance matrices across all the UL and DL users, respectively. As we assume perfect CSI, the SI can be cancelled with HYBF up to the LDR noise level only, which represents the residual SI.

Figure 4 shows the achieved average WSR with the proposed HYBF designs as a function of the LDR noise with SNR = 0 dB. The fully digital FD scheme achieves an additional gain of  $\sim 97\%$  over a fully digital HD scheme. The impact of different LDR noise levels on the maximum achievable WSR for a mmWave FD system with a different number of RF chains at the FD BS is also shown. For  $k_0 \leq$

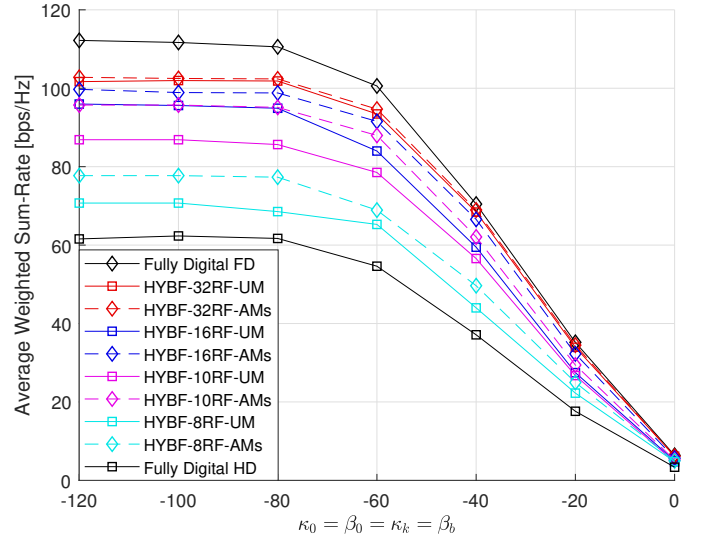


Fig. 5: Average WSR as a function of the LDR noise with SNR = 40 dB.

−40 dB, HYBF-UM and HYBF-AMs achieve an additional gain of  $\sim 85\%, 64\%, 42\%, 3\%$  and  $\sim 89\%, 74\%, 60\%, 28\%$  with 32, 16, 10, 8 RF chains, respectively. We can see that as the LDR noise variance increases, achievable WSR for both the hybrid FD and the fully digital HD system degrades severely. Figure 5 shows the achieved average WSR as a function of the LDR noise with SNR = 40dB. For  $k_0 \leq -80$  dB, HYBF-UM and HYBF-AMs achieve an additional gain of  $\sim 65\%, 55\%, 41\%, 15\%$  and  $\sim 67\%, 62\%, 55\%, 26\%$  with 32, 16, 10, 8 RF chains, respectively, and increasing the LDR noise variance degrades the achieved average WSR. By comparing Figure 4 with Figure 5, we can see that at low SNR, HYBF-UM with only 8 RF chains performs close to the fully digital HD scheme. As the SNR increases to 40 dB, HYBF-UM with 8 RF achieves an additional gain of  $\sim 15\%$ . HYBF-AMs with 8 RF chains outperforms the fully digital HD scheme for all the SNR levels. Figures 4-5 also show that HYBF-AMs with 10 RF chains achieves similar average WSR as the HYBF-UM with 16 RF chains. It is interesting to observe that increasing the SNR from 0 dB to 40 dB decreases the thermal noise variance and the LDR noise variance dominates the noise floor already with  $k_0 = -80$  dB at SNR= 40 dB. For SNR= 0 dB, the LDR noise variance dominates only for  $k_0 > -40$  dB. From this observation, we can conclude that hardware with a low LDR noise is required to benefit from a high SNR in the mmWave FD systems.

Figure 6 shows the average WSR with a low LDR noise level  $\kappa_0 = -80$  dB with 32, 16, 10 and 8 RF chains as a function of the SNR. Both the proposed designs perform very close to the fully digital FD scheme with 32 RF chains. HYBF-UM and HYBF-AMs outperform the fully digital HD scheme with only 8 RF chains at high SNR and at any SNR level, respectively. It is evident the advantage of AMs, which add additional gain for all the SNR levels when the number RF chains at the FD BS is small. With a high number of RF chains, digital beamforming has enough amplitude manipulation lib-

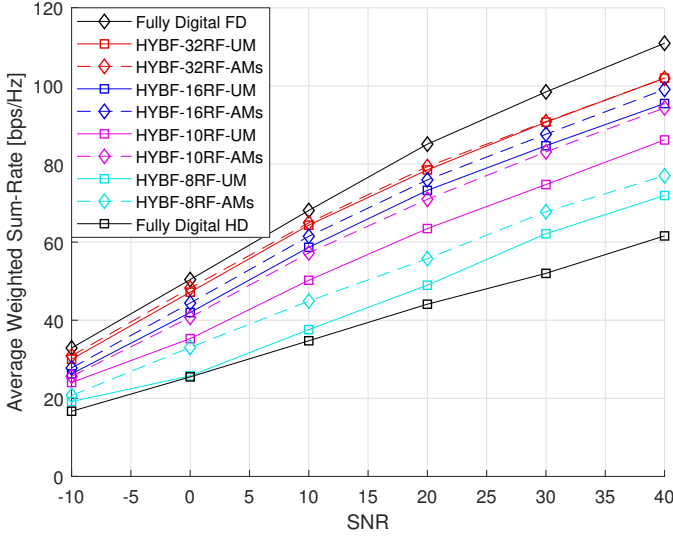


Fig. 6: Average WSR as a function of the SNR with LDR noise  $k_0 = -80$  dB.

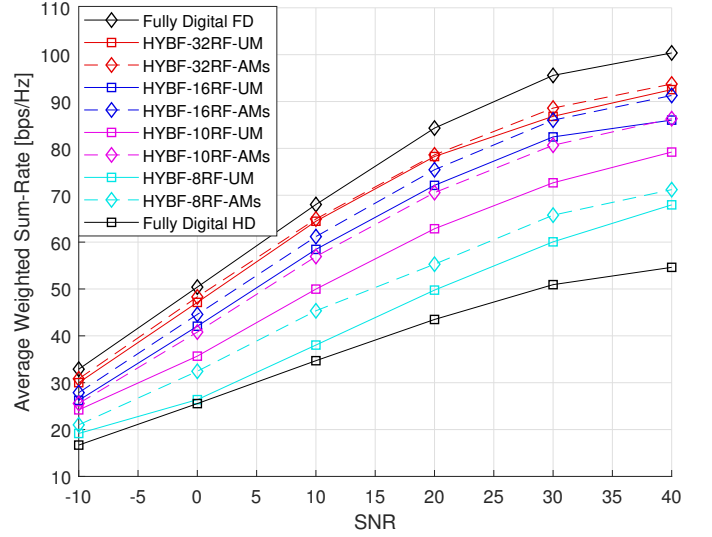


Fig. 7: Average WSR as a function of the SNR with LDR noise  $k_0 = -60$  dB.

erty to manage the interference and adding AMs does not bring further improvement. Figure 7 shows the average WSR achieved with a moderate LDR noise level  $k_0 = -60$  dB. We can see that for a low SNR, the achieved average WSR results to be similar as reported in Figure 6. At high SNR, the LDR noise variance starts dominating, which leads to less achieved average WSR compared to the case of Figure 6. Figure 8 shows the achieved WSR as a function of the SNR with a very large LDR noise variance of  $k_0 = -40$  dB. By comparing the results reported in Figure 8 and Figures 6-7, we can see that the LDR noise variance dominates for most of the considered SNR range. For a very low SNR, the achieved WSR is similar as reported in Figures 6-7. However, as the SNR increases, it does not map into higher WSR. We can see that the maximum achievable WSR with  $k_0 = -40$  dB saturates already at SNR= 20 dB for both the HD and the FD systems. Further improvement in the SNR does not dictate into higher WSR. When the LDR noise variance dominates, it acts as a ceiling to the effective received-signal-to-LDR-plus-thermal-noise-ratio (RSLTR). The transmit and receive LDR noise variance is proportional to the total transmit power per-antenna and received power per RF chain after the analog combining, respectively. When the LDR noise variance is large, the thermal noise variance has a negligible effect on the effective RSLTR. Consequently, a decrease in the thermal noise variance (increasing SNR) does not dictate a better WSR.

Figure 9 shows the achievable performance of the HYBF-UM and the HYBF-AMs schemes as a function of the RF chains with SNR= 20 dB, in comparison with the benchmark schemes, with very high and very small LDR noise levels. In particular, with very high LDR noise  $k_k = -40$  dB and 8 RF chains, HYBF-UM and HYBF-AMs perform close to the fully HD system, and an increase in the number of RF chains improves the performance, which tends towards the achieved WSR by a fully digital FD system with LDR noise level  $k_k = -40$  dB. Similar behaviour can be observed for the case of low

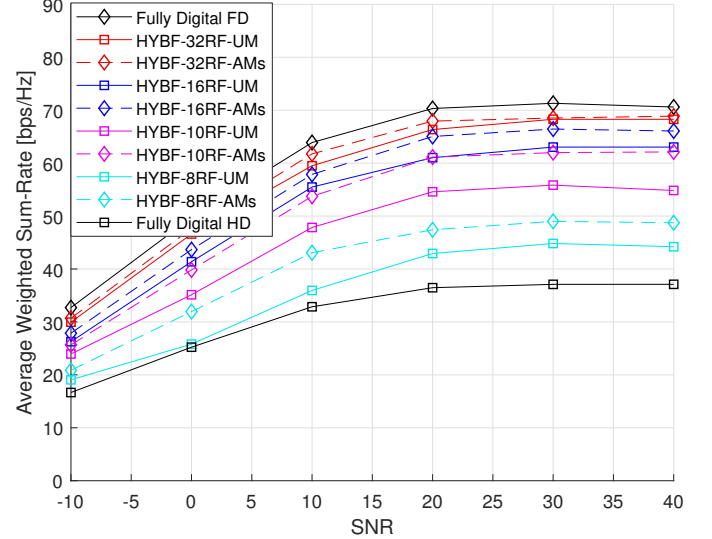


Fig. 8: Average WSR as function of the SNR with LDR noise  $k_0 = -40$  dB.

LDR noise  $k_k = -80$  dB. Both the proposed schemes achieve higher WSR with the same number of RF chains in the latter case. We can also see that AMs add additional gain with a low number of RF chains, and as the number of RF chains increase, the gap in the achievable WSR with HYBF-AMs and HYBF-UM closes. In particular, with 32 RF chains, the difference in the WSR with or without AMs becomes negligible.

From the results reported in Figures 4-9, we can conclude that the proposed HYBF schemes achieve significant performance improvement, in terms of average WSR, compared to a fully digital HD system. LDR noise plays a key role in determining the maximum achievable WSR for both the FD and the HD system. Figures 4-5 showed how an increase in the LDR noise variance degrades the average WSR at the low and high SNR levels. Figures 6-7 showed that with a

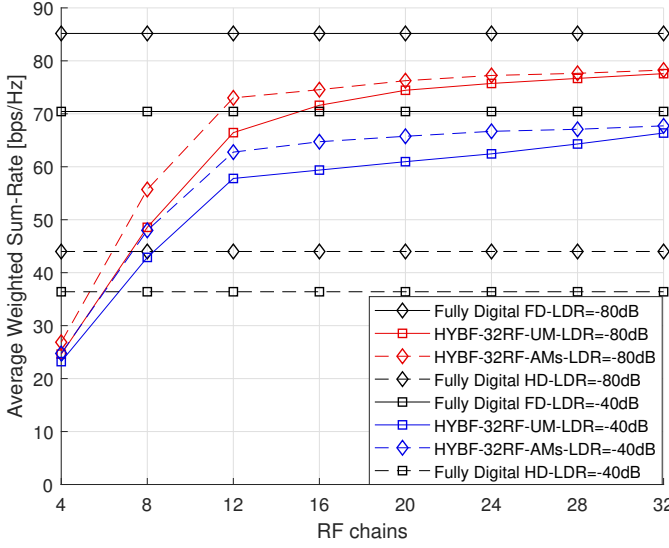


Fig. 9: Average WSR as a function of the RF chains with a very small and a very large LDR noise level at SNR= 20 dB.

large to moderate dynamic range, the LDR noise degrades the performance only at very high SNR. Figure 8 showed the achieved WSR as a function of a very large LDR noise variance. In that case, it is observed that the WSR saturates at SNR= 20 dB and further improvement in the SNR does not dictate higher WSR. Figure 9 showed how the number of RF chains at the mmWave FD BS affects the achievable WSR with different LDR noise levels and with or without the AMs.

## VI. CONCLUSION

This paper has presented a novel HYBF design to maximize the WSR in a single-cell mmWave FD system with multi-antenna users and suffering from LDR noise. The beamformers were designed under the joint sum-power and the practical per-antenna power constraints. Simulation results showed that the multi-user mmWave FD systems can outperform the fully digital HD system with only a few RF chains. The advantage of having amplitude control at the analog processing stage is also investigated, and the benefit was evident with a small number of RF chains. Achievable average WSR with different levels of the LDR noise variance is also investigated, and the proposed HYBF designs outperformed the fully digital HD system at any LDR noise level.

## APPENDIX A GRADIENT DERIVATION

The proof of Theorem 1 is based on the results derived in the following.

**Lemma 3.** Let  $\mathbf{Y} = \mathbf{A}\mathbf{X}\mathbf{B} + a \mathbf{A} \text{diag}(\mathbf{X} + \mathbf{Q})\mathbf{B} + b \text{diag}(\mathbf{C}\mathbf{X}\mathbf{D} + \mathbf{E}) + \mathbf{F}$ . The derivative of  $\ln \det(\mathbf{Y})$  with respect to  $\mathbf{X}$  is given by

$$\frac{\partial \ln \det \mathbf{Y}}{\partial \mathbf{X}} = \mathbf{A}^H \mathbf{Y}^{-H} \mathbf{B}^H + a \text{diag}(\mathbf{A}^H \mathbf{Y}^{-H} \mathbf{B}^H) + b \mathbf{C}^H \text{diag}(\mathbf{Y}^{-H}) \mathbf{D}^H. \quad (40)$$

*Proof.* By substituting  $\phi = \text{Indet}(\mathbf{Y})$ , we can write

$$\partial \phi = \mathbf{Y}^{-H} : d\mathbf{Y} = \text{Tr}(\mathbf{Y}^{-1} d\mathbf{Y}), \quad (41)$$

where operator  $:$  denotes the Frobenius inner product, i.e.  $\mathbf{G}_{RF} : \mathbf{H} = \text{Tr}(\mathbf{G}_{RF}^H \mathbf{H})$ . Its derivative with respect to  $\mathbf{X}$  can be written as

$$\frac{\partial \phi}{\partial \mathbf{X}} = \mathbf{Y}^{-H} : \left[ \frac{d}{d\mathbf{X}} (\mathbf{A}\mathbf{X}\mathbf{B} + a \text{Adiag}(\mathbf{X})\mathbf{B} + b \text{diag}(\mathbf{C}\mathbf{X}\mathbf{D} + \mathbf{E}) + \mathbf{F}) \right], \quad (42)$$

where the last term results to be zero as independent from  $\mathbf{X}$ . Now substituting the Frobenius product with the trace operator and using its cyclic shift property to bring  $\mathbf{X}$  on the right hand side, we have

$$\begin{aligned} \frac{\partial \phi}{\partial \mathbf{X}} &= \underbrace{\frac{\partial \text{Tr}(\mathbf{B}\mathbf{Y}^{-1}\mathbf{A}\mathbf{X})}{\partial \mathbf{X}}}_I + a \underbrace{\frac{\partial \text{Tr}(\mathbf{B}\mathbf{Y}^{-1}\text{Adiag}(\mathbf{X}))}{\partial \mathbf{X}}}_{II} \\ &\quad + b \underbrace{\frac{\partial \text{Tr}(\mathbf{Y}^{-1}\text{diag}(\mathbf{C}\mathbf{X}\mathbf{D}))}{\partial \mathbf{X}}}_{III} + b \frac{\partial \text{Tr}(\mathbf{Y}^{-1}\text{diag}(\mathbf{E}))}{\partial \mathbf{X}}, \end{aligned} \quad (43)$$

where the last term being independent of  $\mathbf{X}$  is also zero. Now we proceed by proving step by step the derivatives for I, II and III. Firstly, for I we have

$$\frac{\partial \text{Tr}(\mathbf{B}\mathbf{Y}^{-1}\mathbf{A}\mathbf{X})}{\partial \mathbf{X}} = \mathbf{A}^H \mathbf{Y}^{-H} \mathbf{B}^H : \partial \mathbf{X} = \mathbf{A}^H \mathbf{Y}^{-H} \mathbf{B}^H. \quad (44)$$

To obtain the derivative of II, let  $\text{diag}(\mathbf{X}) = \mathbf{Z}$ . A diagonal of  $\mathbf{X}$  can be written as  $\text{diag}(\mathbf{X}) = \mathbf{I} \circ \mathbf{X}$  where  $\circ$  denote the Hadamard product. By using its commutative property, we can write

$$\begin{aligned} a \frac{\partial \text{Tr}(\mathbf{B}\mathbf{Y}^{-1}\mathbf{A}\mathbf{Z})}{\partial \mathbf{Z}} &= a \mathbf{A}^H \mathbf{Y}^{-H} \mathbf{B}^H : \partial \mathbf{Z}, \\ &= a \mathbf{A}^H \mathbf{Y}^{-H} \mathbf{B}^H : \mathbf{I} \circ \partial \mathbf{X}, \\ &= a \mathbf{A}^H \mathbf{Y}^{-H} \mathbf{B}^H \circ \mathbf{I} : \partial \mathbf{X}, \\ &= a \text{diag}(\mathbf{A}^H \mathbf{Y}^{-H} \mathbf{B}^H). \end{aligned} \quad (45)$$

To compute the derivative of III, let  $\text{diag}(\mathbf{C}\mathbf{X}\mathbf{D}) = \mathbf{W}$  and by again using the commutative property of the Hadamard product, we have

$$\begin{aligned} b \frac{\partial \text{Tr}(\mathbf{Y}^{-1}\mathbf{W})}{\partial \mathbf{W}} &= b \mathbf{Y}^{-H} : \partial \mathbf{W}, \\ &= b \mathbf{Y}^{-H} : \mathbf{I} \circ \mathbf{C} \partial \mathbf{X} \mathbf{D}, \\ &= b \mathbf{Y}^{-H} \circ \mathbf{I} : \mathbf{C} \partial \mathbf{X} \mathbf{D}, \\ &= b \text{diag}(\mathbf{Y}^{-H}) : \mathbf{C} \partial \mathbf{X} \mathbf{D}, \\ &= b \mathbf{C}^H \text{diag}(\mathbf{Y}^{-1})^H \mathbf{D}^H. \end{aligned} \quad (46)$$

which concludes the proof.  $\square$

To proof the result for Theorem 1, note that the covariance matrices in 11 has a special (Hermitian) structure, i.e.,  $\mathbf{B} = \mathbf{A}^H$  and  $\mathbf{D} = \mathbf{C}^H$ . Therefore, the result of Lemma 3 for this particular is given in the Lemma stated in the following.

**Lemma 4.** Let  $\mathbf{Y} = \mathbf{A}\mathbf{X}\mathbf{B} + a \text{Adiag}(\mathbf{X} + \mathbf{Q})\mathbf{B} + b \text{diag}(\mathbf{C}\mathbf{X}\mathbf{D} + \mathbf{E}) + \mathbf{F}$ , where the size of matrices involved



is such that the product is valid. Let  $\mathbf{B} = \mathbf{A}^H$  and  $\mathbf{D} = \mathbf{C}^H$  and the derivative of  $\ln \det(\mathbf{Y})$  is given by

$$\frac{\partial \ln \det \mathbf{Y}}{\partial \mathbf{X}} = \mathbf{A}^H \mathbf{Y}^{-H} \mathbf{A} + a \operatorname{diag}(\mathbf{A}^H \mathbf{Y}^{-H} \mathbf{A}) + b \mathbf{C}^H \operatorname{diag}(\mathbf{Y}^{-H}) \mathbf{C}. \quad (47)$$

*Proof.* The result follows directly by relying on the result given in Lemma 3 by substituting  $\mathbf{B} = \mathbf{A}^H$  and  $\mathbf{D} = \mathbf{C}^H$   $\square$

*Proof. Theorem 1* To prove the gradients to linearize the WSR with respect to  $\mathbf{T}_k$  and  $\mathbf{Q}_j$ , we proceed by simplifying the WSR as

$$\begin{aligned} \text{WSR} &= \sum_{k \in \mathcal{U}} w_k \ln \det(\mathbf{R}_k) - w_k \ln \det(\mathbf{R}_{\bar{k}}) \\ &+ \sum_{j \in \mathcal{D}} w_j \ln \det(\mathbf{R}_j) - w_j \ln \det(\mathbf{R}_{\bar{j}}). \end{aligned} \quad (48)$$

The  $\text{WSR}_{\bar{k}}^{UL}$  and  $\text{WSR}_{\bar{j}}^{DL}$  should be linearized for  $\mathbf{T}_k$  and  $\text{WSR}_{\bar{j}}^{DL}$  and  $\text{WSR}_{\bar{k}}^{UL}$  for  $\mathbf{Q}_j$ . Note from (11) that  $\mathbf{T}_k$  appears in  $\text{WSR}_{\bar{k}}^{UL}$  and  $\text{WSR}_{\bar{k}}^{DL}$  with the structure  $\mathbf{Y} = \mathbf{A} \mathbf{X} \mathbf{A}^H + a \mathbf{A} \operatorname{diag}(\mathbf{X} + \mathbf{Q}) \mathbf{A}^H + b \operatorname{diag}(\mathbf{C} \mathbf{X} \mathbf{C}^H + \mathbf{E}) + \mathbf{F}$ , where the scalars  $a$  and  $b$  are due to the LDR noise model,  $\mathbf{A}$  and  $\mathbf{C}$  are the interfering channels,  $\mathbf{F}$  and  $\mathbf{E}$  contain the noise contributions from other transmit covariance matrices but independent from  $\mathbf{T}_k$ . The same structure holds also for the DL covariance matrices  $\mathbf{Q}_j, \forall j \in \mathcal{D}$ . By applying the result from Lemma 4 with  $\mathbf{Y} = \mathbf{R}_k$  or  $\mathbf{Y} = \mathbf{R}_{\bar{k}}$  repetitively  $K-1$  time for linearizing  $\text{WSR}_{\bar{k}}^{UL}$  with respect to  $\mathbf{T}_k$  yield the gradient  $\mathbf{A}_k$ . Similarly, by considering  $\mathbf{Y} = \mathbf{R}_j$  or  $\mathbf{Y} = \mathbf{R}_{\bar{j}}, \forall j \in \mathcal{D}$  applying the results from Lemma 4 yield the gradient  $\mathbf{B}_k$ .

The same reasoning holds for  $\mathbf{Q}_j$ , which leads to the gradients  $\hat{\mathbf{C}}_j$  and  $\hat{\mathbf{D}}_j$  by applying the result provided in Lemma 4 for  $\text{WSR}_{\bar{j}}^{DL}$   $J-1$  times and for  $\text{WSR}_{\bar{k}}^{UL}$   $K$  times, respectively,  $\forall j \in \mathcal{D}$ .  $\square$

## APPENDIX B PROOF OF THEOREM 3

The dominant generalized eigenvector solution maximizes the reformulated concave WSR maximization problem

$$\begin{aligned} \text{WSR} &= \sum_{k \in \mathcal{U}} w_k \ln \det(\mathbf{I} + \mathbf{U}_k^H \mathbf{H}_k^H \mathbf{F}_{RF} \mathbf{R}_k^{-1} \mathbf{F}_{RF}^H \mathbf{H}_k \mathbf{U}_k) \\ &- \operatorname{Tr}(\mathbf{U}_k^H (\hat{\mathbf{A}}_k + \hat{\mathbf{B}}_k + l_k \mathbf{I} + \mathbf{\Psi}_k) \mathbf{U}_k) \\ &+ \sum_{j \in \mathcal{D}} w_j \ln \det(\mathbf{I} + \mathbf{V}_j^H \mathbf{G}_{RF}^H \mathbf{H}_j^H \mathbf{R}_j^{-1} \mathbf{H}_j \mathbf{G}_{RF} \mathbf{V}_j) \\ &- \operatorname{Tr}(\mathbf{V}_j^H \mathbf{G}_{RF}^H (\hat{\mathbf{C}}_j + \hat{\mathbf{D}}_j + l_0 \mathbf{I} + \mathbf{\Psi}_0) \mathbf{G}_{RF} \mathbf{V}_j). \end{aligned} \quad (49)$$

To prove the results stated in Theorem 3 to solve (49), we first consider the UL digital beamforming solution by keeping the analog beamformer and the digital DL beamformers fixed. For the optimal digital UL beamforming solution, we consider

user  $k \in \mathcal{U}$ . However, the same proof is valid for  $\forall k \in \mathcal{U}$ . It relies on simplifying

$$\begin{aligned} \max_{\mathbf{U}_k} \quad & w_k \ln \det(\mathbf{I} + \mathbf{U}_k^H \mathbf{H}_k^H \mathbf{F}_{RF} \mathbf{R}_k^{-1} \mathbf{F}_{RF}^H \mathbf{H}_k \mathbf{U}_k) \\ & - \operatorname{Tr}(\mathbf{U}_k^H (\hat{\mathbf{A}}_k + \hat{\mathbf{B}}_k + l_k \mathbf{I} + \mathbf{\Psi}_k) \mathbf{U}_k) \end{aligned} \quad (50)$$

until the Hadamard's inequality applies as in Proposition 1 [57] or Theorem 1 [59]. The Cholesky decomposition of the matrix  $(\hat{\mathbf{A}}_k + \hat{\mathbf{B}}_k + l_k \mathbf{I} + \mathbf{\Psi}_k)$  is given as  $\mathbf{L}_k \mathbf{L}_k^H$  where  $\mathbf{L}_k$  is the lower triangular Cholesky factor. By defining  $\tilde{\mathbf{U}}_k = \mathbf{L}_k^H \mathbf{U}_k$ , (50) reduces to

$$\begin{aligned} \max_{\mathbf{U}_k} \quad & w_k \ln \det(\mathbf{I} + \tilde{\mathbf{U}}_k^H \mathbf{L}_k^{-1} \mathbf{H}_k^H \mathbf{F}_{RF} \mathbf{R}_k^{-1} \mathbf{F}_{RF}^H \mathbf{H}_k \\ & \mathbf{L}_k^{-H} \tilde{\mathbf{U}}_k) - \operatorname{Tr}(\tilde{\mathbf{U}}_k^H \tilde{\mathbf{U}}_k). \end{aligned} \quad (51)$$

Let  $\mathbf{E}_k \mathbf{D}_k \mathbf{E}_k^H$  be the eigen-decomposition of  $\mathbf{L}_k^{-1} \mathbf{H}_k^H \mathbf{R}_k^{-1} \mathbf{H}_k \mathbf{L}_k^{-H}$ , where  $\mathbf{E}_k$  and  $\mathbf{D}_k$  are the unitary and diagonal matrices, respectively. Let  $\mathbf{O}_k = \mathbf{E}_k^H \tilde{\mathbf{U}}_k \tilde{\mathbf{U}}_k^H \mathbf{E}_k$ , the (51) can be expressed as

$$\max_{\mathbf{O}_k} \quad w_k \ln \det(\mathbf{I} + \mathbf{O}_k \mathbf{D}_k) - \operatorname{Tr}(\mathbf{O}_k). \quad (52)$$

By Hadamard's inequality [Page 233 [60]], it can be seen that the optimal  $\mathbf{O}_k$  must be diagonal. Therefore,  $\mathbf{U}_k = \mathbf{L}_k^{-H} \mathbf{E}_k \mathbf{O}_k^{\frac{1}{2}}$  and thus

$$\begin{aligned} \mathbf{H}_k^H \mathbf{F}_{RF} \mathbf{R}_k^{-1} \mathbf{F}_{RF}^H \mathbf{H}_k \mathbf{U}_k &= \mathbf{L}_k \mathbf{L}_k^H \mathbf{L}_k^{-H} \mathbf{E}_k \mathbf{O}_k^{\frac{1}{2}} \mathbf{D}_k \\ &= (\hat{\mathbf{A}}_k + \hat{\mathbf{B}}_k + l_k \mathbf{I} + \mathbf{\Psi}_k) \mathbf{U}_k \mathbf{D}_k, \end{aligned} \quad (53)$$

from which we select  $u_k$  dominant eigenvectors and it concludes the proof for the UL beamformer for user  $k \in \mathcal{U}$ . For the digital DL beamformers the proof follow similarly.

$$\begin{aligned} \max_{\mathbf{V}_j} \quad & w_j \ln \det(\mathbf{I} + \mathbf{V}_j^H \mathbf{G}_{RF}^H \mathbf{H}_j^H \mathbf{R}_j^{-1} \mathbf{H}_j \mathbf{G}_{RF} \mathbf{V}_j) \\ & - \operatorname{Tr}(\mathbf{V}_j^H \mathbf{G}_{RF}^H (\hat{\mathbf{C}}_j + \hat{\mathbf{D}}_j + l_0 \mathbf{I} + \mathbf{\Psi}_0) \mathbf{G}_{RF} \mathbf{V}_j). \end{aligned} \quad (54)$$

and simplifying it until the Hadamard's inequality applies to yield a result as expressed in (53).

The proof for the analog beamformer does not apply directly as the KKT conditions have the form  $\mathbf{A}_1 \mathbf{G}_{RF} \mathbf{A}_2 = \mathbf{B}_1 \mathbf{G}_{RF} \mathbf{B}_2$ . To solve it for the analog beamformer  $\mathbf{G}_{RF}$ , we apply the result  $\operatorname{vec}(\mathbf{A} \mathbf{X} \mathbf{B}) = \mathbf{B}^T \otimes \operatorname{Avec}(\mathbf{X})$  [61], which allows to rewrite (22) as

$$\begin{aligned} \sum_{j \in \mathcal{D}} w_j \left( \left( \mathbf{V}_j \mathbf{V}_j^H (\mathbf{I} + \mathbf{V}_j \mathbf{V}_j^H \mathbf{G}_{RF}^H \mathbf{H}_j^H \mathbf{R}_j^{-1} \mathbf{H}_j \mathbf{G}_{RF}) \right)^{-1} \right)^T \otimes \\ \mathbf{H}_j^H \mathbf{R}_j^{-1} \mathbf{H}_j \operatorname{vec}(\mathbf{G}_{RF}) - \sum_{j \in \mathcal{D}} \left( (\mathbf{V}_j \mathbf{V}_j^H)^T \otimes (\hat{\mathbf{C}}_j \right. \\ \left. + \hat{\mathbf{D}}_j + \mathbf{\Psi}_0 + l_0 \mathbf{I}) \right) \operatorname{vec}(\mathbf{G}_{RF}) = 0. \end{aligned} \quad (55)$$

The analog beamformer solution can alternatively be derived as follows (which allows the proof above to be applicable directly). First we apply a noise whitening procedure using the noise plus interference covariance matrix  $\mathbf{R}_{\bar{j}}^{1/2}$  on the received

signal. Further, we can rewrite the whitened signal as follows

$$\tilde{\mathbf{y}}_j = \left( (\mathbf{s}_{jd}^T \mathbf{V}_j^T) \otimes \mathbf{R}_j^{-1/2} \mathbf{H}_j \right) \text{vec}(\mathbf{G}_{RF}) + \tilde{\mathbf{n}}_j, \quad (56)$$

where  $\tilde{\mathbf{y}}_j = \mathbf{R}_j^{-1/2} \mathbf{y}_j$  and  $\tilde{\mathbf{n}}_j$  represents the whitened noise plus interference signal. Further, we can write the resulting WSR optimization problem (after the approximation to concave form and some algebraic manipulations on the linearized term) as

$$\begin{aligned} \max_{\mathbf{G}_{RF}} \quad & \sum_{j \in \mathcal{D}} w_j \ln \det \left( \mathbf{I} + \text{vec}(\mathbf{G}_{RF})^H \left( (\mathbf{V}_j \mathbf{V}_j^H)^T \otimes \mathbf{H}_j^H \mathbf{R}_j^{-1} \right. \right. \\ & \left. \left. \mathbf{H}_j \right) \text{vec}(\mathbf{G}_{RF}) \right) - \text{Tr} \left( \text{vec}(\mathbf{G}_{RF})^H \left( \mathbf{V}_j \mathbf{V}_j^H \otimes \right. \right. \\ & \left. \left. (\hat{\mathbf{C}}_j + \hat{\mathbf{D}}_j) + \Psi_0 + l_0 \mathbf{I} \right) \text{vec}(\mathbf{G}_{RF}) \right). \end{aligned} \quad (57)$$

Further, taking the gradient for  $\mathbf{G}_{RF}$  leads to the same generalized eigenvector solution as in (23). Also, note that this alternative representation has the same form as (50). Hence, the proof for the UL and DL digital beamformers can now be applied directly on the vectorized analog beamformer  $\text{vec}(\mathbf{G}_{RF})$ , which is summed over all the DL users.

#### ACKNOWLEDGMENT

The research leading to these results received funding from the French National Research Agency (ANR) via the DUPLEX project. EURECOMs research is also partially supported by its industrial members: ORANGE, BMW, Symantec, SAP, Monaco Telecom, iABG, by the projects MASS-START (French FUI) and EU ITN project SPOTLIGHT.

#### REFERENCES

- [1] Z. Pi and F. Khan, "An introduction to millimeter-wave mobile broadband systems," *IEEE Communications Magazine*, vol. 49, no. 6, pp. 101–107, Jun. 2011.
- [2] S. Rangan, T. S. Rappaport, and E. Erkip, "Millimeter-wave cellular wireless networks: Potentials and challenges," *Proceedings of the IEEE*, vol. 102, no. 3, pp. 366–385, Mar. 2014.
- [3] S. Liu, L. Fu, and W. Xie, "Hidden-node problem in full-duplex enabled CSMA networks," *IEEE Transactions on Mobile Computing*, vol. 19, no. 2, pp. 347–361, Jan. 2019.
- [4] H. Alves, T. Riihonen, and H. A. Suraweera, *Full-Duplex Communications for Future Wireless Networks*. Springer, 2020.
- [5] M. T. Kabir and C. Masouros, "A scalable energy vs. latency trade-off in full-duplex mobile edge computing systems," *IEEE Transactions on Communications*, vol. 67, no. 8, pp. 5848–5861, May 2019.
- [6] C. B. Barneto, S. D. Liyanaarachchi, M. Heino, T. Riihonen, and M. Valkama, "Full duplex radio/radar technology: The enabler for advanced joint communication and sensing," *IEEE Wireless Communications*, vol. 28, no. 1, pp. 82–88, Feb. 2021.
- [7] M. Gan, Y. Guo, G. Tsodik, Y. Xin, X. Yang, E. Au, and O. Aboul-Magd, "Full duplex for next generation of 802.11," in *IEEE 30th International Symposium on Personal, Indoor and Mobile Radio Communications (PIMRC Workshops)*, Sep. 2019, pp. 1–6.
- [8] P. Rosson, C. K. Sheemar, N. Valecha, and D. Slock, "Towards massive MIMO in-band full duplex radio," in *IEEE 16th International Symposium on Wireless Communication Systems (ISWCS)*, Aug. 2019, pp. 69–74.
- [9] S. Huberman and T. Le-Ngoc, "MIMO full-duplex precoding: A joint beamforming and self-interference cancellation structure," *IEEE Transactions on Wireless Communications*, vol. 14, no. 4, pp. 2205–2217, Apr. 2014.
- [10] P. Aquilina, A. C. Cirik, and T. Ratnarajah, "Weighted sum rate maximization in full-duplex multi-user multi-cell MIMO networks," *IEEE Transactions on Communications*, vol. 65, no. 4, pp. 1590–1608, Apr. 2017.
- [11] T. Riihonen and R. Wichman, "Analog and digital self-interference cancellation in full-duplex MIMO-OFDM transceivers with limited resolution in A/D conversion," in *IEEE 46th Asilomar Conference on Signals, Systems and Computers (ASILOMAR)*, Nov. 2012, pp. 45–49.
- [12] B. P. Day, A. R. Margetts, D. W. Bliss, and P. Schniter, "Full-duplex bidirectional MIMO: Achievable rates under limited dynamic range," *IEEE Transactions on Signal Processing*, vol. 60, no. 7, pp. 3702–3713, Apr. 2012.
- [13] O. Taghizadeh, J. Zhang, and M. Haardt, "Transmit beamforming aided amplify-and-forward MIMO full-duplex relaying with limited dynamic range," *Signal Processing*, vol. 127, pp. 266–281, Mar. 2016.
- [14] A. C. Cirik, S. Biswas, S. Vuppala, and T. Ratnarajah, "Beamforming design for full-duplex MIMO interference channels-QoS and energy-efficiency considerations," *IEEE Transactions on Communications*, vol. 64, no. 11, pp. 4635–4651, Nov. 2016.
- [15] E. Antonio-Rodríguez, R. López-Valcarce, T. Riihonen, S. Werner, and R. Wichman, "SINR optimization in wideband full-duplex MIMO relays under limited dynamic range," in *IEEE 8th Sensor Array and Multichannel Signal Processing Workshop (SAM)*, Jun. 2014, pp. 177–180.
- [16] S. Biswas, K. Singh, O. Taghizadeh, and T. Ratnarajah, "Design and analysis of FD MIMO cellular systems in coexistence with MIMO radar," *IEEE Transactions on Wireless Communications*, vol. 19, no. 7, pp. 4727–4743, Jul. 2020.
- [17] A. C. Cirik, O. Taghizadeh, L. Lampe, R. Mathar, and Y. Hua, "Linear transceiver design for full-duplex multi-cell MIMO systems," *IEEE Access*, vol. 4, pp. 4678–4689, Sep. 2016.
- [18] O. Taghizadeh, V. Radhakrishnan, A. C. Cirik, R. Mathar, and L. Lampe, "Hardware impairments aware transceiver design for bidirectional full-duplex MIMO OFDM systems," *IEEE Transactions on Vehicular Technology*, vol. 67, no. 8, pp. 7450–7464, Aug. 2018.
- [19] T. Schenk, *RF Imperfections in High-rate Wireless Systems: Impact and Digital Compensation*. Springer Science & Business Media, Jan. 2008.
- [20] S. R. Aghdam, S. Jacobsson, and T. Eriksson, "Distortion-aware linear precoding for millimeter-wave multiuser MISO downlink," in *IEEE International Conference on Communications Workshops (ICC Workshops)*, May 2019, pp. 1–6.
- [21] H. Abbas and K. Hamdi, "Full duplex relay in millimeter wave backhaul links," in *IEEE Wireless Communications and Networking Conference*, Apr. 2016, pp. 1–6.
- [22] R. López-Valcarce and N. González-Prelcic, "Analog beamforming for full-duplex millimeter wave communication," in *16th International Symposium on Wireless Communication Systems (ISWCS)*, Aug. 2019, pp. 687–691.
- [23] S. Han, Y. Zhang, W. Meng, C. Li, and Z. Zhang, "Full-duplex relay-assisted macrocell with millimeter wave backhauls: Framework and prospects," *IEEE Network*, vol. 33, no. 5, pp. 190–197, Oct. 2019.
- [24] C. K. Sheemar and D. T. Slock, "Hybrid beamforming for bidirectional massive MIMO full duplex under practical considerations," in *IEEE 93rd Vehicular Technology Conference (VTC) Spring*, Apr. 2021.
- [25] K. Satyanarayana, M. El-Hajjar, P.-H. Kuo, A. Mourad, and L. Hanzo, "Hybrid beamforming design for full-duplex millimeter wave communication," *IEEE Transactions on Vehicular Technology*, vol. 68, no. 2, pp. 1394–1404, Dec. 2018.
- [26] Y. Cai, K. Xu, A. Liu, M. Zhao, B. Champagne, and L. Hanzo, "Two-timescale hybrid analog-digital beamforming for mmwave full-duplex mimo multiple-relay aided systems," *IEEE Journal on Selected Areas in Communications*, vol. 38, no. 9, pp. 2086–2103, Jun. 2020.
- [27] S. Huang, Y. Ye, and M. Xiao, "Learning based hybrid beamforming design for full-duplex millimeter wave systems," *IEEE Transactions on Cognitive Communications and Networking*, vol. 7, pp. 120–132, Mar. 2020.
- [28] C. K. Thomas, C. K. Sheemar, and D. Slock, "Multi-stage/hybrid BF under limited dynamic range for OFDM FD backhaul with MIMO SI nulling," in *IEEE 16th International Symposium on Wireless Communication Systems (ISWCS)*, Aug. 2019, pp. 96–101.
- [29] E. Balti, N. Mensi, and S. Yan, "A modified zero-forcing max-power design for hybrid beamforming full-duplex systems," *arXiv preprint arXiv:2003.00147*, 2020.
- [30] M.-M. Zhao, Y. Cai, M.-J. Zhao, Y. Xu, and L. Hanzo, "Robust joint hybrid analog-digital transceiver design for full-duplex mmwave multicell systems," *IEEE Transactions on Communications*, vol. 68, no. 8, pp. 4788–4802, Aug. 2020.
- [31] J. M. B. da Silva, A. Sabharwal, G. Fodor, and C. Fischione, "1-bit phase shifters for large-antenna full-duplex mmwave communications," *IEEE Transactions on Wireless Communications*, vol. 19, no. 10, pp. 6916–6931, Oct. 2020.



- [32] I. P. Roberts, J. G. Andrews, and S. Vishwanath, "Hybrid beamforming for millimeter wave full-duplex under limited receive dynamic range," *arXiv preprint arXiv:2012.11647*, 2020.
- [33] J. Palacios, J. Rodriguez-Fernandez, and N. González-Prelcic, "Hybrid precoding and combining for full-duplex millimeter wave communication," in *IEEE Global Communications Conference (GLOBECOM)*, Dec. 2019, pp. 1–6.
- [34] I. P. Roberts and S. Vishwanath, "Beamforming cancellation design for millimeter-wave full-duplex," in *IEEE Global Communications Conference (GLOBECOM)*, Dec. 2019, pp. 1–6.
- [35] I. P. Roberts, H. B. Jain, and S. Vishwanath, "Equipping millimeter-wave full-duplex with analog self-interference cancellation," in *IEEE International Conference on Communications Workshops (ICC Workshops)*, Jun. 2020, pp. 1–6.
- [36] C. K. Sheemar and D. Slock, "Hybrid beamforming and combining for millimeter wave full duplex massive MIMO interference channel," *arXiv preprint arXiv:2108.00465*, 2021.
- [37] I. P. Roberts, H. B. Jain, and S. Vishwanath, "Frequency-selective beamforming cancellation design for millimeter-wave full-duplex," in *IEEE International Conference on Communications (ICC)*, Jun. 2020, pp. 1–6.
- [38] C. K. Sheemar and D. Slock, "Massive MIMO mmwave full duplex relay for IAB with limited dynamic range," in *IEEE 11th IFIP International Conference on New Technologies, Mobility and Security (NTMS)*, Apr. 2021, pp. 1–5.
- [39] D. Korpi, T. Riihonen, V. Syrjälä, L. Anttila, M. Valkama, and R. Wichman, "Full-duplex transceiver system calculations: Analysis of ADC and linearity challenges," *IEEE Transactions on Wireless Communications*, vol. 13, no. 7, pp. 3821–3836, Apr. 2014.
- [40] C. K. Sheemar, L. Badia, and S. Tomasin, "Game-theoretic mode scheduling for dynamic TDD in 5G systems," *IEEE Communications Letters*, vol. 25, no. 7, pp. 2425 – 2429, Apr. 2021.
- [41] J. M. B. da Silva, G. Wikström, R. K. Mungara, and C. Fischione, "Full duplex and dynamic TDD: Pushing the limits of spectrum reuse in multi-cell communications," *IEEE Wireless Communications*, vol. 28, no. 1, pp. 44–50, Feb. 2021.
- [42] H. Kim, J. Kim, and D. Hong, "Dynamic TDD systems for 5G and beyond: A survey of cross-link interference mitigation," *IEEE Communications Surveys & Tutorials*, vol. 22, no. 4, pp. 2315–2348, Jul. 2020.
- [43] E. de Olivindo Cavalcante, G. Fodor, Y. C. Silva, and W. C. Freitas, "Bidirectional sum-power minimization beamforming in dynamic TDD MIMO networks," *IEEE Transactions on Vehicular Technology*, vol. 68, no. 10, pp. 9988–10002, Aug. 2019.
- [44] S. Guo, X. Hou, and H. Wang, "Dynamic TDD and interference management towards 5G," in *IEEE Wireless Communications and Networking Conference (WCNC)*, Apr. 2018, pp. 1–6.
- [45] P. Stoica and Y. Selen, "Cyclic minimizers, majorization techniques, and the expectation-maximization algorithm: A refresher," *IEEE Signal Processing Magazine*, vol. 21, no. 1, pp. 112–114, Feb. 2004.
- [46] E. G. Larsson, O. Edfors, F. Tufvesson, and T. L. Marzetta, "Massive MIMO for next generation wireless systems," *IEEE Communications Magazine*, vol. 52, no. 2, pp. 186–195, Feb. 2014.
- [47] W. Yu and T. Lan, "Transmitter optimization for the multi-antenna downlink with per-antenna power constraints," *IEEE Transactions on Signal Processing*, vol. 55, no. 6, pp. 2646–2660, May 2007.
- [48] T. Lan and W. Yu, "Input optimization for multi-antenna broadcast channels with per-antenna power constraints," in *IEEE Global Telecommunications Conference (GLOBECOM)*, Nov. 2004, pp. 420–424.
- [49] R. Chaluviadi, S. S. Nair, and S. Bhashyam, "Optimal multi-antenna transmission with multiple power constraints," *IEEE Transactions on Wireless Communications*, vol. 18, no. 7, pp. 3382–3394, Apr. 2019.
- [50] C. K. Sheemar and D. T. Slock, "Beamforming for bidirectional MIMO full duplex under the joint sum power and per antenna power constraints," in *IEEE International Conference on Acoustics, Speech and Signal Processing (ICASSP)*, Jun. 2021, pp. 4800–4804.
- [51] A. C. Cirik, O. Taghizadeh, L. Lampe, R. Mathar, and Y. Hua, "Linear transceiver design for full-duplex multi-cell MIMO systems," *IEEE Access*, vol. 4, pp. 4678–4689, Aug. 2016.
- [52] M. R. Castellanos, V. Raghavan, J. H. Ryu, O. H. Koymen, J. Li, D. J. Love, and B. Peleato, "Hybrid multi-user precoding with amplitude and phase control," in *IEEE International Conference on Communications (ICC)*, May 2018, pp. 1–6.
- [53] M. Majidzadeh, J. Kaleva, N. Tervo, H. Pennanen, A. Tölli, and M. Latva-Aho, "Rate maximization for partially connected hybrid beamforming in single-user MIMO systems," in *IEEE 19th International Workshop on Signal Processing Advances in Wireless Communications (SPAWC)*, Jun. 2018, pp. 1–5.
- [54] L. Chen, A. Liu, and X. Yuan, "Structured turbo compressed sensing for massive MIMO channel estimation using a Markov prior," *IEEE Transactions on Vehicular Technology*, vol. 67, no. 5, pp. 4635–4639, Dec. 2017.
- [55] I. P. Roberts, J. G. Andrews, H. B. Jain, and S. Vishwanath, "Millimeter-wave full duplex radios: New challenges and techniques," *IEEE Wireless Communications*, vol. 28, no. 1, pp. 36–43, Feb. 2021.
- [56] "Weighted sum-rate maximization using weighted MMSE for MIMO-BC beamforming design," *IEEE Transactions on Wireless Communications*, vol. 7, no. 12, pp. 4792–4799, Dec. 2008.
- [57] S.-J. Kim and G. B. Giannakis, "Optimal resource allocation for MIMO ad hoc cognitive radio networks," *IEEE Transactions on Information Theory*, vol. 57, no. 5, pp. 3117–3131, Apr. 2011.
- [58] S. P. Boyd and L. Vandenberghe, *Convex Optimization*. Cambridge university press, 2004.
- [59] D. Hoang and R. A. Iltis, "Noncooperative eigencoding for MIMO ad-hoc networks," *IEEE Transactions on Signal Processing*, vol. 56, no. 2, pp. 865–869, Jan. 2008.
- [60] T. M. Cover and J. A. Thomas, *Elements of Information Theory*. John Wiley & Sons, 1991.
- [61] J. R. Magnus and H. Neudecker, *Matrix Differential Calculus with Applications in Statistics and Econometrics*. John Wiley & Sons, 2019.